Finite Size Scaling Analysis of Ising Model Block Distribution Functions

K. Binder

Institut für Festkörperforschung, Kernforschungsanlage Jülich,
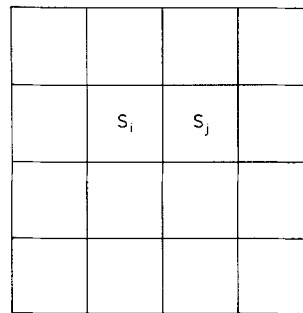Jülich, Federal Republic of Germany

The distribution function $P_L(s)$ of the local order parameters in finite blocks of linear dimension L is studied for Ising lattices of dimensionality $d = 2, 3$ and 4. Apart from the case where the block is a subsystem of an infinite lattice, also the distribution in finite systems with free $[P_L^{(f)}(s)]$ and periodic $[P_L^{(p)}(s)]$ boundary conditions is treated. Above the critical point T_c, these distributions tend for large L towards the same gaussian distribution centered around zero block magnetization, while below T_c these distributions tend towards two gaussians centered at $\pm M$, where M is the spontaneous magnetization appearing in the infinite systems. However, below T_c the wings of the distribution at small $|s|$ are distinctly nongaussian, reflecting two-phase coexistence. Hence the distribution functions can be used to obtain the interface tension between ordered phases.

At criticality, the distribution functions tend for large L towards scaled universal forms, though dependent on the boundary conditions. These scaling functions are estimated from Monte Carlo simulations. For subsystem-blocks, good agreement with previous renormalization group work of Bruce is obtained.

As an application, it is shown that Monte Carlo studies of critical phenomena can be improved in several ways using these distribution functions: (i) standard estimates of order parameter, susceptibility, interface tension are improved (ii) T_c can be estimated independent of critical exponent estimates (iii) A Monte Carlo "renormalization group" similar to Nightingale's phenomenological renormalization is proposed, which yields fairly accurate exponent estimates with rather moderate effort (iv) Information on coarse-grained hamiltonians can be gained, which is particularly interesting if the method is extended to more general Hamiltonians.

I. Introduction

In the statistical mechanics of many-body systems, it is a familiar concept to divide the system in "cells" or "blocks" of finite linear dimension L. This concept has been applied to understand phase coexistence in the van der Waals fluid [1], to derive scaling laws between critical exponents [2], and to justify the use of a coarse-grained free energy functional useful for both the description of nucleation and spinodal decomposition [3–5], and as a starting point for the renormalization group theory of critical phenomena [6–9]. For a d-dimensional Ising system, the magnetization s_i of the i'th cell (cf. Fig. 1) can be defined as

Fig. 1. Division of the system into blocks of linear dimension L, s_i representing the degrees of freedom of the i-th block

$$s_i = (1/L^d) \sum_{l \in i'\text{th cell}} S_l, \qquad S_l = \pm 1. \qquad (1)$$

It is then assumed that the Boltzmann factor $(1/Z)\exp[-\mathcal{H}_{\text{Ising}}/k_B T]$, with

$$\mathcal{H}_{\text{Ising}} = -\sum_{l \neq l'} J_{ll'} S_l S_{l'} - H\sum_l S_l, \qquad (2)$$

where $J_{ll'}$ are the exchange constants between spins at lattice sites l, l', and H is the magnetic field, is replaced by the probability for the field s_i,

$$P_L(\{s_i\}) = (1/Z)\exp[-\mathcal{H}_{\text{GLW}}(\{s_i\})]. \qquad (3)$$

Here factors of $1/k_B T$ are for convenience absorbed in the coefficients of the Ginzburg-Landau-Wilson Hamiltonian $\mathcal{H}_{\text{GLW}}(\{s_i\})$, which usually is expanded as

$$\mathcal{H}_{\text{GLW}}(\{s_i\}) = \sum_i (h_L s_i + r_L s_i^2 + u_L s_i^4 + v_L s_i^6 + \ldots)$$
$$+ \sum_{\langle i,j \rangle} C_L(s_i - s_j)^2 + \ldots, \qquad (4)$$

with $h_L, r_L, u_L, v_L, \ldots, C_L, \ldots$ appropriate coefficients, and $\langle i,j \rangle$ denotes a summation over nearest-neighbor cells (Fig. 1). In order that an expansion such as (4) is valid, where only low-order terms are kept and the coefficients $r_L, u_L, v_L, \ldots, C_L, \ldots$ depend on temperature (and other external parameters) in a non-singular way, it is crucial that $L \ll \xi$, the correlation length of order parameter fluctuations [5-8]. Close enough to T_c, where ξ is arbitrarily large, one can choose $L \gg 1$ (measuring lengths in units of the lattice spacing) at the same time, and one can proceed further, replacing (4) by a continuum approximation.

Although the step from (2) to (4) is of crucial conceptual importance, it is hardly ever carried out explicitly. Thus, the parameters $r_L, u_L, v_L, \ldots, C_L, \ldots$ can not be explicitly related to the parameters of the microscopic hamiltonian (exchange constants $J_{ll'}$ in the present example). Hence the resulting theories of critical behavior (and also of first-order transition kinetics [4]) can predict the universal properties of the system only, information on non-universal properties is lost. In more complicated cases it may happen, that the same type of hamiltonian can exhibit critical behavior belonging to different universality classes, depending on the values of the interaction parameters. Then the renormalization group analysis of the resulting coarse-grained hamiltonian $\mathcal{H}_{\text{GLW}}$ will exhibit several (nontrivial) fixed points [7] – but it may be unclear to which of them a particular given hamiltonian belongs.

While it is hardly possible to perform the above coarse-graining exactly, it is possible to obtain at least explicit numerical results by Monte Carlo methods [9], sampling the distribution function $P_L(\{s_i\})$. As a first step of such a program, the present paper studies the reduced distribution function of one block,

$$P_L(s_i) = \int \prod_{j \neq i} ds_j P_L(\{s_j\}). \qquad (5)$$

In addition, we consider the related distribution functions of finited systems of linear dimension L, such as $P_L^{(f)}(s)$ for isolated blocks with free boundary conditions and $P_L^{(p)}(s)$ for isolated blocks with periodic boundary conditions. Section II describes some general results on these functions, including properties for $L \gg \xi$, which is a situation not normally considered in the renormalization group approach. A scaling assumption, which can be justified by the latter [10], is exploited. Section III presents numerical results, and the resulting universal scaling functions are estimated. In addition, it is shown how these distribution functions can be used to obtain improved estimates of order parameter, susceptibility, and interface tension, i.e. quantities often obtained by standard Monte Carlo analysis in a different way. Section IV then proposes to use the distribution functions to construct a phenomenological "Monte Carlo renormalization group (MCRG)", similar to Nightingale's finite size renormalization group [11-13]. As an example, this method is applied to Ising lattices for $d = 2, 3$ and 4 dimensions, and we compare our approach to other versions of MCRG [14-23]. Section V contains our conclusions, and briefly discusses generalizations to other systems.

II. General Properties of the Block Distribution Functions

We consider the situation where the magnetic field $H = 0$. Then $\mathcal{H}_{\text{Ising}}$ (2) is symmetric with respect to a change of sign of all the spins, and hence we obtain a symmetric block distribution function

$$P_L(s) = P_L(-s). \qquad (6)$$

Above T_c we then have, from (1)

$$\langle s^2 \rangle_L = L^{-2d} \sum_{l,l' \in i'\text{th cell}} \langle S_l S_{l'} \rangle_T \equiv L^{-d} k_B T \chi_L, \qquad (7)$$

where χ_L is an estimate for the susceptibility χ of the total system

$$k_B T \chi = \frac{1}{N} \sum_{l,l'} \langle S_l S_{l'} \rangle_T, \qquad N \to \infty, \quad T > T_c. \qquad (8)$$

It is clear that for values of L much larger than the correlation length ξ of the order-parameter correlation function $\langle S_l S_{l'}\rangle_T$ the difference between χ_L and χ will be small, involving only boundary terms of relative magnitude $\sim L^{-1}$,

$$\chi_L = \chi - \chi_b L^{-1}, \quad L \gg \xi. \tag{9}$$

Of course, similar relations are already familiar for finite systems with periodic or free boundary conditions [24]; for subblocks, however, the significance of χ_b is different.

Next we consider the higher moments and cumulants of the distribution, which we denote as U_L, V_L, etc.,

$$\langle s^k \rangle_L = \int ds\, s^k P_L(s), \quad k = 2, 4, 6, \ldots, \tag{10}$$

$$U_L = 1 - \langle s^4 \rangle_L / (3 \langle s^2 \rangle_L^2), \tag{11}$$

$$V_L = 1 - \langle s^4 \rangle_L / (2 \langle s^2 \rangle_L^2) + \langle s^6 \rangle_L / (30 \langle s^2 \rangle_L^3), \ldots \tag{12}$$

Since

$$\langle s^4 \rangle_L = L^{-4d} \sum_{l,l',l'',l''' \in i'^{\text{ih}} \text{cell}} \langle S_l S_{l'} S_{l''} S_{l'''} \rangle$$

$$= 3 \langle s^2 \rangle_L^2 + L^{-4d} \sum_{l l' l'' l'''} (\langle S_l S_{l'} S_{l''} S_{l'''} \rangle$$

$$- \langle S_l S_{l'} \rangle \langle S_{l''} S_{l'''} \rangle - \langle S_l S_{l''} \rangle \langle S_{l'} S_{l'''} \rangle$$

$$- \langle S_l S_{l'''} \rangle \langle S_{l'} S_{l''} \rangle) \equiv 3 \langle s^2 \rangle_L^2 - L^{-3d} (k_B T) \chi_L^{(2)}. \tag{13}$$

One finds that

$$U_L \equiv L^{-d} \chi_L^{(2)} / 3 \chi_L^2 \xrightarrow[L \to \infty]{} L^{-d} \chi^{(2)} / 3 \chi^2, \tag{14}$$

where $\chi^{(2)} = \lim_{L \to \infty} \chi_L^{(2)}$ is defined in terms of (13). For large L, thus $U_L \propto L^{-d}$, and similarly one finds that V_L vanishes proportional to L^{-2d} for large L, etc. Away from the critical point, the correlation length ξ is finite, and hence the "susceptibilities" $\chi_L, \chi_L^{(2)}$, etc. tend to finite values for $L \to \infty$. As expected, all cumulants become negligible for large L, and $P_L(s)$ is a gaussian

$$P_L(s) = L^{d/2} (2\pi k_B T \chi_L)^{-1/2} \exp[-s^2 L^d / (2 k_B T \chi_L)],$$

or $\hfill (15\text{a})$

$$P_L(s) \approx L^{d/2} (2\pi k_B T \chi)^{-1/2} \exp[-s^2 L^d / (2 k_B T \chi)]. \tag{15b}$$

Of course, this result could have been justified at once referring to the central limit theorem of probability theory [25], but here we are interested also in the deviations from gaussian behavior, as measured by (11)–(14).

Below T_c a spontaneous magnetization $\pm M$ appears in the thermodynamic limit, and any state with a spontaneous magnetization does no longer have the

symmetry property (6). Rather we must distinguish the probability $P_L^{(+)}(s)$ for finding the block magnetization s in a block L^d for positive spontaneous magnetization from the probability $P_L^{(-)}(s)$ for negative magnetization, and (6) is replaced by

$$P_L^{(+)}(s) = P_L^{(-)}(-s). \tag{16}$$

In the following we are interested in the symmetrized distribution,

$$P_L^{(s)}(s) = [P_L(s) + P_L(-s)]/2, \quad T < T_c, \tag{17}$$

which no longer distinguishes the sign of the magnetization. The reason for this choice is that it can be meaningfully compared to the distributions of finite systems $\{P_L^{(f)}(s) \text{ and } P_L^{(p)}(s)$, as introduced above$\}$, for which there is no spontaneous magnetization. Thus also for arbitrarily large but finite N (6) still holds, and $P_L(s)$ smoothly develops towards $P_L^{(s)}(s)$ [rather than either $P_L^{(+)}(s)$ or $P_L^{(-)}(s)$] for $N \to \infty$. The block magnetization $\langle |s| \rangle_L$,

$$\langle |s| \rangle = \int_{-\infty}^{+\infty} ds |s| P_L^{(s)}(s) = L^{-d} \sum_{l \in i'^{\text{ih}} \text{cell}} \langle |S_l| \rangle_T \tag{18}$$

then tends smoothly towards the spontaneous magnetization M as $N \to \infty$, and similar to (7) one can define a susceptibility χ_L,

$$k_B T \chi_L = L^d (\langle s^2 \rangle_L - \langle |s| \rangle_L^2) \xrightarrow[L \to \infty]{} k_B T \chi$$

$$= \sum_{i (\neq j)} [\langle S_i S_j \rangle_T - M^2], \quad T < T_c. \tag{19}$$

Thus, although there is never a spontaneous magnetization in a finite system, there is no difficulty in estimating both M and χ for $T < T_c$, as long as $L \gg \xi$. Of course, this fact has been utilized in Monte Carlo calculations for a long time already [26].

From the fact that $k_B T \chi$ for $T < T_c$ is finite, we conclude that the "variance" $\langle s^2 \rangle_L - \langle |s| \rangle_L^2 \approx k_B T \chi / L^d$ is very small for $L \gg \xi$, and hence $P_L(s)$ must be sharply peaked at $s \approx \pm \langle |s| \rangle_L$. To leading order, the cumulant U_L then becomes

$$U_L \approx \tfrac{2}{3} - \tfrac{4}{3} \langle |s| \rangle_L^{-2} L^{-d} k_B T \chi_L + O(L^{-2d}), \tag{20}$$

and similarly V_L tends towards $V_\infty = 8/15$.

As a first attempt of constructing $P_L(s)$ for $T < T_c$ explicitly, it is tempting to use two displaced gaussians,

$$P_L(s) \cong \tfrac{1}{2} L^{d/2} (2\pi k_B T \chi_L)^{-1/2}$$

$$\{\exp[-(s - \langle |s| \rangle_L)^2 L^d / (2 k_B T \chi_L)]$$

$$+ \exp[-(s + \langle |s| \rangle_L)^2 L^d / (2 k_B T \chi_L)]\}. \tag{21}$$

It must be realized, however, that (21) represents the
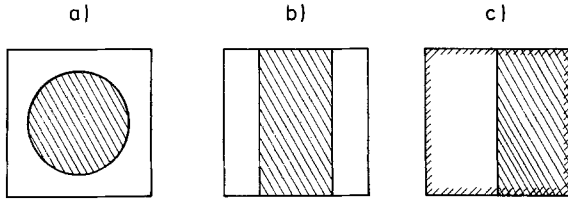
a)   b)   c)

Fig. 2. Typical configurations of twodimensional blocks for $L \gg \xi$, $s \approx 0$, in the cases where the block is a subsystem of a large system (a) or where it is an isolated finite system with periodic (b) or free (c) boundary conditions. Shaded areas indicate domains of negative magnetization, white areas have positive magnetization

distribution reasonably even for $L \gg \xi$ only near the peaks of the distribution, but not in its wings. In the regime $-\langle |s| \rangle_L \ll s \ll +\langle |s| \rangle_L$ (21) underestimates distinctly the actual $P_L(s)$. This fact is appreciated by noting that in this regime $P_L(s)$ will be dominated by configurations corresponding to two-phase coexistence within the cell L^d, Fig. 2. Consider for the moment finite blocks with free or periodic boundary conditions. Their free energy is given by

$$Z_L = \exp[-F_L(H)/k_B T] \equiv Tr \exp[-\mathscr{H}/k_B T]$$

$$= \int\limits_{-\infty}^{-\infty} ds \exp[-F_L(s)/k_B T + HL^d s/k_B T], \qquad (22)$$

where we have allowed for $H \neq 0$, and $F(s)$ is defined by the constrained partition function [27]

$$\exp[-F_L(s)/k_B T]$$

$$= Tr \exp\left[\frac{J}{k_B T} \sum_{\langle l, l' \rangle} S_l S_{l'}\right] \delta(sL^d - \sum_l S_l). \qquad (23)$$

The probability distributions $P_L^{(p,f)}(s)$ hence can be related to the constrained free energy $F(s)$,

$$P_L^{(p,f)}(s) = \exp[-F_L^{(p,f)}(s)/k_B T]/Z_L \qquad (24)$$

Also $P_L(s)$ can be associated to a free energy $F_L(s)$ of a finite block which is the subsystem of a large system. The free energies $F_L(s)$, $F_L^{(p)}(s)$ and $F_L^{(f)}(s)$ have their minima at S_{max} where $P_L(s)$ is maximal, which is in the vicinity of $s = \pm M$, while the free energy cost of having states with $s \approx 0$ is due to interface contributions [27,28]. For large enough subsystem blocks, the free energy $F_L(s \approx 0)$ will be dominated by the domain configuration which has the minimum interface area, which is a spherical domain. We estimate the radius R of this domain putting

$$L^d/2 = V_d R^d, \qquad (25)$$

denoting volume (and surface area) of the d-dimensional unit sphere by V_d (and S_d, respectively). Hence

the surface area of the domain in Fig. 2a is estimated as

$$A = S_d \left(\frac{|M - s|}{2MV_d}\right)^{(d-1)/d} L^{d-1}, \qquad (26)$$

and thus we estimate the free energy cost of the domain in Fig. 2a (for $H = 0$) as

$$F_L(s \approx 0) - F_L(s = s_{max}) = Af_s = S_d \left(\frac{|M - s|}{2MV_d}\right)^{(d-1)/d} L^{d-1} f_s, \qquad (27)$$

where f_s is an appropriate surface tension. Since the interface entropy of a finite spherical droplet is expected to differ from that of an infinite planar interface [28], f_s is itself expected to be weakly dependent on L.

For $F_L^{(p)}(s)$ the minimum free energy excess is again needed for the spherical domain configuration as long as $|s| > s_{crit}$

$$s_{crit} = M[1 - 2V_d(2/S_d)^{d/(d-1)}]$$

$$= \begin{cases} M(1 - 2/\pi) \approx 0.363M & (d = 2) \\ M(1 - 4/(3(2\pi)^{1/2})) \approx 0.468M & (d = 3) \end{cases} \qquad (28)$$

while for $|s| < s_{crit}$ the minimum free energy excess is obtained for a rectangular domain extending throughout the block, making use of the periodic boundary condition. While (27) then again holds for $|s| > s_{crit}$, for $|s| < s_{crit}$ it is replaced by [see Fig. 2b]

$$F_L(s \approx 0) - F_L(s - s_{max}) = 2L^{d-1} f_s^{(p)}, \qquad (28)$$

which is independent of s. The surface tension which enters in (28) will again depend weakly on L, since contributions of fluctuations with wavelengths exceeding L are not contributing to it due to the periodic boundary condition. Similarly, the minimum free energy excess for $F^{(f)}(s)$ is again needed for the spherical domain configuration as long as $|s| > s'_{crit}$,

$$s'_{crit} = M[1 - 2V_d(1/S_d)^{d/(d-1)}]$$

$$= \begin{cases} M\left(1 - \frac{1}{2\pi}\right) \approx 0.841M & (d = 2) \\ M\left(1 - \frac{2}{3(4\pi)^{1/2}}\right) \approx 0.812M & (d = 3), \end{cases} \qquad (29)$$

while for $|s| < s'_{crit}$ the minimum free energy excess is obtained by creating just one wall, Fig. 2c, and hence

$$F_L(s \approx 0) - F_L(s = s_{max}) = L^{d-1} f_s^{(f)}. \qquad (30)$$

In this expression, it is assumed that the free surface contributions to $F(s \approx 0)$ and $F(s = s_{max})$, which would

be also of order L^{d-1}, are essentially the same and thus cancel out. We expect that

$$\lim_{L\to\infty} f_s(L) = \lim_{L\to\infty} f_s^{(p)}(L) = \lim_{L\to\infty} f_s^{(f)}(L) = F_s, \qquad (31)$$

with F_s being the usual interface tension between two phases of opposite magnetization separated by an infinitely large interface. Equations (24), (31) suggest that the asymptotic decay of $P_L(s)$ for $-M \ll s \ll +M$ is given by $\exp(-\text{const} L^{d-1})$ rather than $\exp(-\text{const} L^d)$ as suggested by the two-gaussian approximation (21). In addition (31) suggests that $P_L(s)$ can be used to estimate the interface tension F_s.

Next we turn to the behavior of $P_L(s)$ in the immediate vicinity of the critical point. We assume that for $T \to T_c$ and $L \to \infty P_L(s)$ satisfies a finite size scaling hypothesis, analogous to usual finite size scaling assumptions [29]

$$P_L(s) = L^x \hat{P} \tilde{P}(a s L^y, \xi/L), \qquad (32)$$

where $\hat{P}$ and a are constants setting the scales for the variables, $\tilde{P}(z,z')$ is a universal scaling function, and the exponents x, y will be estimated below [30]. Equation (32) is equivalent to scaling assumptions for multispin-correlation functions, which enter the moments of $P_L(s)$ as discussed above, and which are more familiar from the literature [2, 31]. Although the scaled universal structure of (32) can also be justified from renormalization group arguments [10], doubts in (32) can be raised on the grounds of a possible violation of hyperscaling relations for the three-dimensional Ising model [32, 33]. If one accepts these arguments indicating what might go wrong in applying field theory to the Ising model, one would expect that "weak scaling" theories [34] apply, which "allow for the possibility that one or more additional lengths, such as the width of the interfacial boundary between two coexisting phases, become important in the critical region" [33]. As we have argued above that $P_L(s)$ directly reflects interfacial phenomena, the structure of (32) would be more complicated.

We use here (32) as a working hypothesis and exploit its properties. First we note that the normalization of probability relates the constants $\hat{P}$ and a, as well as the exponents x and y

$$1 \equiv \int_{-\infty}^{+\infty} ds P_L(s) = L^x \hat{P} \int_{-\infty}^{+\infty} ds \tilde{P}(a s L^y, \xi/L)$$

$$= L^{x-y} \frac{\hat{P}}{a} \int_{-\infty}^{+\infty} dz \tilde{P}(z, \xi/L). \qquad (33)$$

We conclude $x = y$ and note that the (universal) function $\int_{-\infty}^{+\infty} dz \tilde{P}(z, \xi/L)$ must acutally be a constant,

which then also is universal, $C_0 = \int_{-\infty}^{+\infty} dz \tilde{P}(z, \infty)$. Thus

$$\hat{P} = a/C_0. \qquad (34)$$

Next we calculate the moments $\langle s^k \rangle_L$ as

$$\langle s^k \rangle_L = L^y \frac{a}{C_0} \int_{-\infty}^{+\infty} ds s^k \tilde{P}(a s L^y, \xi/L)$$

$$= L^{-ky}(a^k C_0)^{-1} \int_{-\infty}^{+\infty} dz z^k \tilde{P}(z, \xi/L)$$

$$\equiv L^{-ky}(a^k C_0)^{-1} f_k(\xi/L), \qquad (35)$$

and thus define (universal) functions $f_k(\xi/L)$. Matching this expression with (7), (9) we conclude that $f_2(\xi/L) = c_2(\xi/L)^{\gamma/\nu}$ for $\xi/L \to 0$, as $\chi \propto \xi^{\gamma/\nu}$ for $T \to T_c$. Thus we find, matching the powers of L,

$$d = \frac{\gamma}{\nu} - 2y, \qquad y = \frac{d\nu - \gamma}{2\nu} = \frac{\beta}{\nu}. \qquad (36)$$

Here the hyperscaling relation $d\nu = \gamma + 2\beta$ is explicitly used. Next we consider the cumulant

$$U_L = 1 - C_0 \frac{f_4(\xi/L)}{3 f_2^2(\xi/L)} \xrightarrow{T \to T_c} U^* \equiv 1 - \frac{C_0 f_4(\infty)}{3 f_2^2(\infty)}, \qquad (37)$$

which is a universal function of ξ/L in the critical region and tends to a universal finite constant, which is nontrivial in contrast to the limiting behavior for $L \to \infty$ off T_c. Similar universal properties hold for the higher order cumulants, too.

Comparing (32), (15b) we find that for $\xi/L \ll 1$ $\tilde{P}(z, z')$ takes the form

$$\tilde{P}(z, z') = \frac{C_0}{\sqrt{\pi}} z'^{-\gamma/2\nu} \exp(-z^2 z'^{-\gamma/\nu}), z' \to 0, \qquad (38)$$

the scale factor a being related to the critical amplitudes $\hat{\chi}^+$ and $\hat{\xi}^+$ of susceptibility and correlation length $[\chi = \hat{\chi}^+ (T/T_c - 1)^{-\gamma}, \xi = \hat{\xi}^+ (T/T_c - 1)^{-\nu}]$ as

$$a = [(\hat{\xi}^+)^{\gamma/\nu} (2 k_B T_c \hat{\chi}^+)^{-1}]^{1/2}. \qquad (39)$$

Below T_c a comparison of (32), (21) yields, for $z' \to 0$,

$$\tilde{P}(z, z') = \frac{C_0 A_1}{2\sqrt{\pi}} z'^{-\gamma/2\nu} \{\exp[-A_1^2 z'^{-d}(z z'^{\beta/\nu} - A_2)^2]$$

$$+ \exp[-A_1^2 z'^{-d}(z z'^{\beta/\nu} + A_2)^2]\}, \qquad (40)$$

which is valid in the regime where either $|z z'^{\beta/\nu} - A_2| \lesssim z'^{d/2}/A_1$ or $|z z'^{\beta/\nu} + A_2| \lesssim z'^{d/2}/A_1$, respectively. The universal constants A_1, A_2 can again be expressed in terms of critical amplitudes $[\chi = \hat{\chi}^- (1 - T/T_c)^{-\gamma}, \xi = \hat{\xi}^- (1 - T/T_c)^{-\nu}, M = \hat{M}(1 - T/T_c)^{\beta}]$ as

$$A_1 = \sqrt{\frac{\hat{\chi}^+}{\hat{\chi}^-}\left(\frac{\hat{\xi}^+}{\hat{\xi}^-}\right)^{-\gamma/\nu}}, \qquad A_2 = \hat{M}(\hat{\xi}^-)^{\beta/\nu} a. \tag{41}$$

In the normalization of (21), (40) it is assumed that the wings of the distribution – where these equations are no longer valid due to the phase coexistence phenomena as discussed above – make a negligible contribution to the area under $P_L(s)$, for $z'= \xi/L \to 0$.

Finally we compare (32) to the expression

$$P_L(0) = P_L(s_{max})$$
$$\exp[-S_d(2V_d)^{-(d-1)/d}L^{d-1}F_s/k_BT], \xi/L \to 0, \tag{42}$$

which follows from (24), (27) and where (21) yields $P_L(s_{max}) = L^{d/2}(2\pi k_B T\chi)^{-1/2}/2$. In this limit $\tilde{P}(0, z')$ becomes

$$\tilde{P}(0, z') = \frac{C_0 A_1}{2\sqrt{\pi}} z'^{-\gamma/2\nu} \exp[-A_3(z')^{1-d}], z' \to 0, \tag{43}$$

the (universal) constant A_3 being related to the critical amplitude of the interface tension $\{F_s/k_B T_c = \hat{F}_s(1-T/T_c)^{(d-1)\nu}\}$ as

$$A_3 = \hat{F}_s S_d[2V_d/(\hat{\xi}^-)^d]^{-(d-1)/d}. \tag{44}$$

III. Monte Carlo Results for Block Distribution Functions of Ising Systems at Two, Three- and Four Dimensions

By standard Monte Carlo simulation [9] $P_L(s)$ was obtained for a variety of temperatures in the critical region for Ising square, cubic and hypercubic lattices of linear dimension $N = 60 (d=2)$, $N = 24 (d=3)$ and $N = 12 (d=4)$, respectively. Periodic boundary conditions were used throughout. The possible values of L consistent with these choices of N are $L = 2, 3, 4, 5, 6, 10, 12, 15, 20, 30$ $(d=2)$; $L = 2, 4, 6, 8, 12$ $(d=3)$; $L = 2, 3, 4, 6$ $(d=4)$. For $d=3$, we have also obtained $P_L^{(f)}(s)$ and $P_L^{(p)}(s)$, for all L from $L=2$ to $L=12$. $P_L^{(f)}(s)$ and $P_L^{(p)}(s)$ are less convenient for Monte Carlo study, since each choice of L requires a separate run, while the above set of subsystem-block sizes is generated in one run simultaneously. We feel that a study of subsystem blocks should also be advantageous for standard Monte Carlo finite size scaling analysis [10, 24, 35], where one tries to fit magnetization M_L (and other observables) of finite blocks to scaling forms such as $M_L(T) = \hat{M}(1-T/T_c)^\beta \tilde{M}\{L(1-T/T_c)^\nu\}$, by simultaneously adjusting the exponents β, ν and T_c such that the set of curves $M_L(T)/(1-T/T_c)^\beta$ falls onto a single curve $\tilde{M}$: The analysis of Sect. II shows that a scaling of this type holds for

the subsystems of a large system as well, and hence one can obtain all the requested information from one run for a sufficiently large system. Every single spin flip in the system yields an event for all studied block sizes simultaneously. Since the system contains $(N/L)^d$ blocks, the number of Monte Carlo steps (MCS)/spin contributing to $P_L(s)$ is enhanced by the factor $(N/L)^d$ in comparison to that for the total system. Thus a number of about 10^4 MCS/spin for the total system yielded rather satisfactory accuracy, while for $P_L^{(f)}(s)$ and $P_L^{(p)}(s)$ about $10^5 - 10^6$ MCS/spin were needed to reach comparable accuracy. Still the results presented below are based on a total computing effort which is more than an order of magnitude less than what is needed for other simulation purposes (such as polymer studies [36], etc.) – thus it would be feasible to even improve the precision of the results significantly.

Figures 3 and 4 show typical "raw data" of the simulation for $P_L(s)$ [38] at $d=2$ and $d=3$ (Results for $d=4$, as well as results for $P_L^{(p)}(s)$ and $P_L^{(f)}(s)$ are qualitatively similar). Below T_c a distinct peak develops increasing in size with L, as expected. The shape of this peak is rather asymmetric, reflecting the expected structure due to two-phase coexistence for $s < M$. This will be analyzed in more detail below. For $d=2$, a double-peaked structure results even at temperatures slightly above T_c, for not too large L. For temperatures far above T_c, there is a single peak at $s=0$; but even then the distribution does not resemble a gaussian for small L.

Of course, in an Ising system $P_L(s)$ as defined by (1), (3) is defined only at a set of discrete points s_k,

$$s_k = 1 - 2k/L^d, \qquad k = 0, 1, ..., L^d. \tag{45}$$

Thus the curves drawn in Figs. 2, 3 through the values $P_L(s_k)$ are just smooth continuations of the points to guide the eye. Remarkably enough, even for small L very smooth functions result from this continuation, and hence it is clearly reasonable to approximate the actual quasi-continuous $P_L(s_k)$ by a continuous function, as done in Sect. II. In addition, for large L the weight of $P_L(s_k)$ at $s_k = \pm 1$ becomes negligibly small, and then it is legitimate to replace the limits of integration $\int_{-1}^{+1} ds...$ by $\int_{-\infty}^{+\infty} ds...$, as done above.

The insert of Fig. 4b illustrates the use of the block distribution for obtaining a more reliable estimate for the spontaneous magnetization appearing in the thermodynamic limit: One obtains sequences of estimates $\langle |s|\rangle_L, \sqrt{\langle s^2\rangle_L}, ...,$ as well as $(s_{max})_L$, which all must extrapolate towards the same value M for $L \to \infty$. The fact that such extrapolations yield results
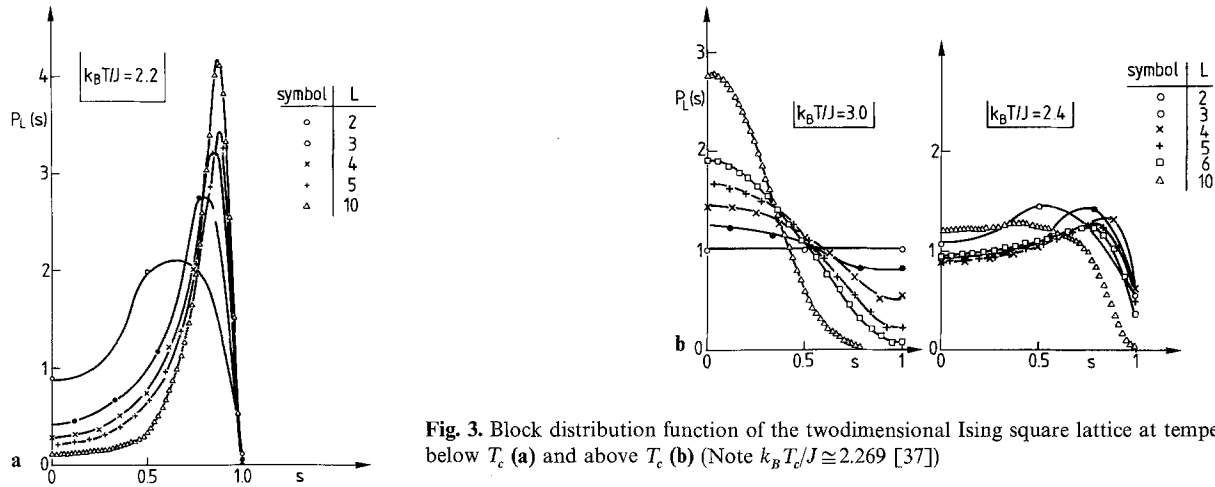
Fig. 3. Block distribution function of the twodimensional Ising square lattice at temperatures below T_c (a) and above T_c (b) (Note $k_B T_c/J \cong 2.269$ [37])
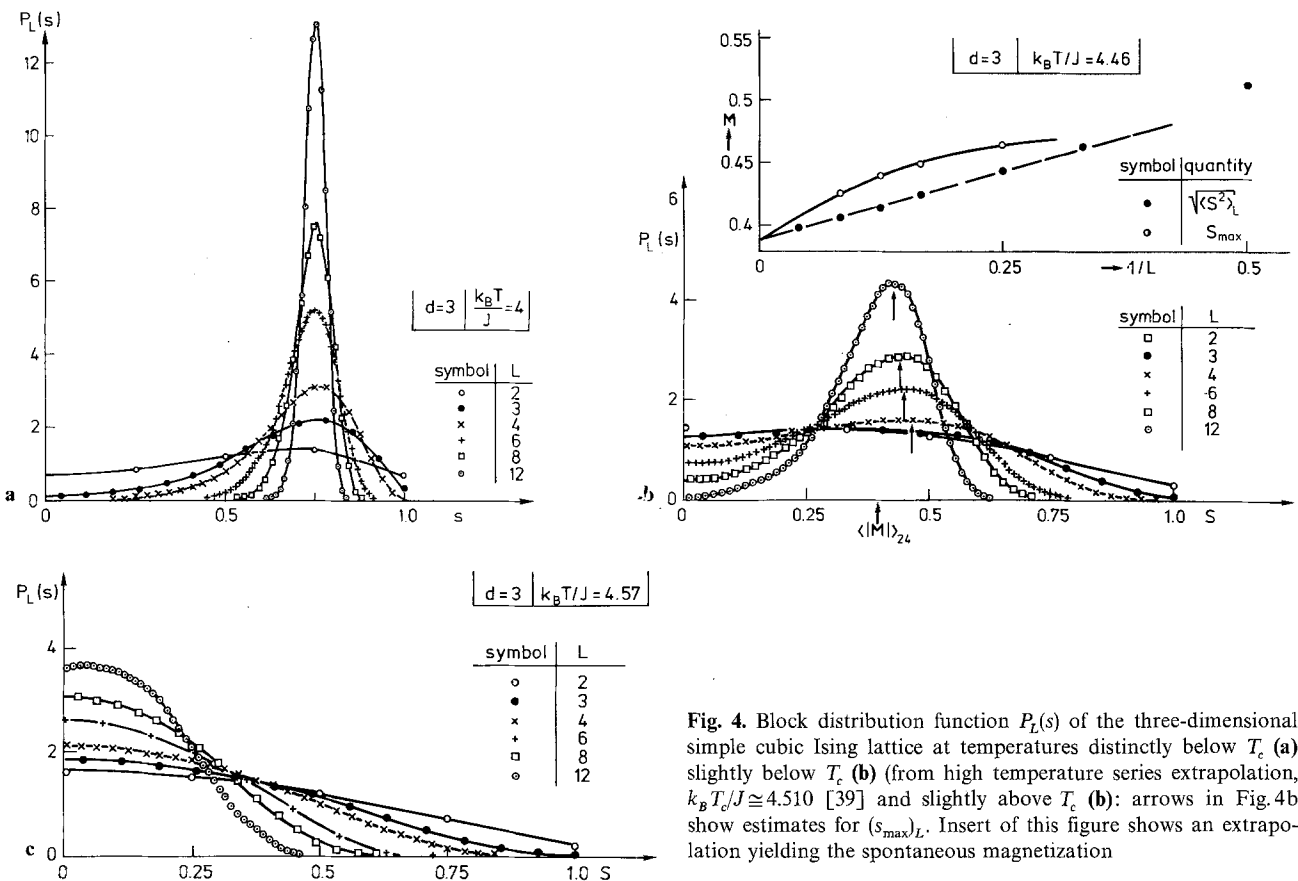

Fig. 4. Block distribution function $P_L(s)$ of the three-dimensional simple cubic Ising lattice at temperatures distinctly below T_c (a) slightly below T_c (b) (from high temperature series extrapolation, $k_B T_c/J \cong 4.510$ [39] and slightly above T_c (b): arrows in Fig. 4b show estimates for $(s_{max})_L$. Insert of this figure shows an extrapolation yielding the spontaneous magnetization

consistent with each other is an important consistency check on the accuracy of the calculation, and gives an idea of finite size effects also for temperatures farther away from T_c, where a standard finite size scaling analysis is not warranted. We also note that very close to T_c (or above T_c) spurious nonzero estimates for M result from finite lattices, because

both $\langle |s| \rangle$, and $\sqrt{\langle s^2 \rangle_L}$ then differ from zero appreciably due to the broad width of the distribution. In this case extrapolation of $(s_{max})_L$ may yield more reliable results.

Figure 5 shows various ways to estimate the susceptibility using the knowledge on the block distribution function. Above T_c, one may either use $\langle s^2 \rangle_L$
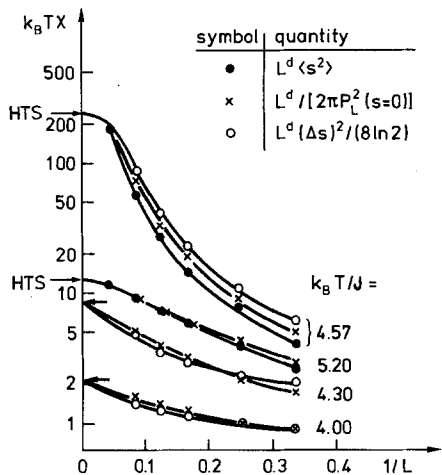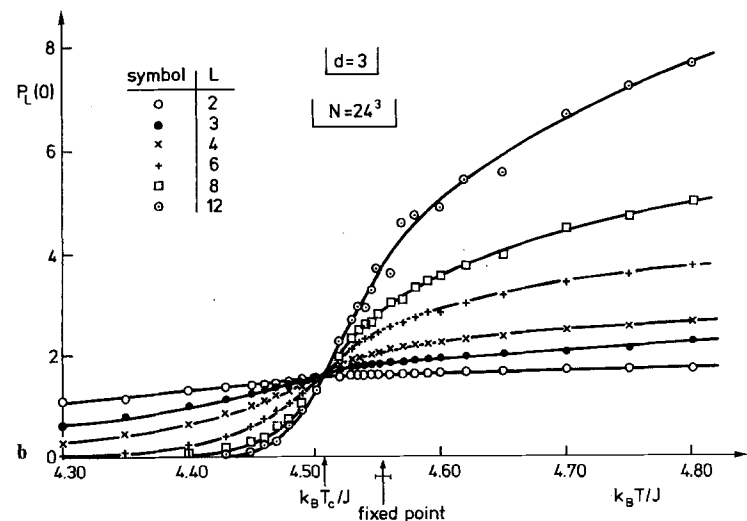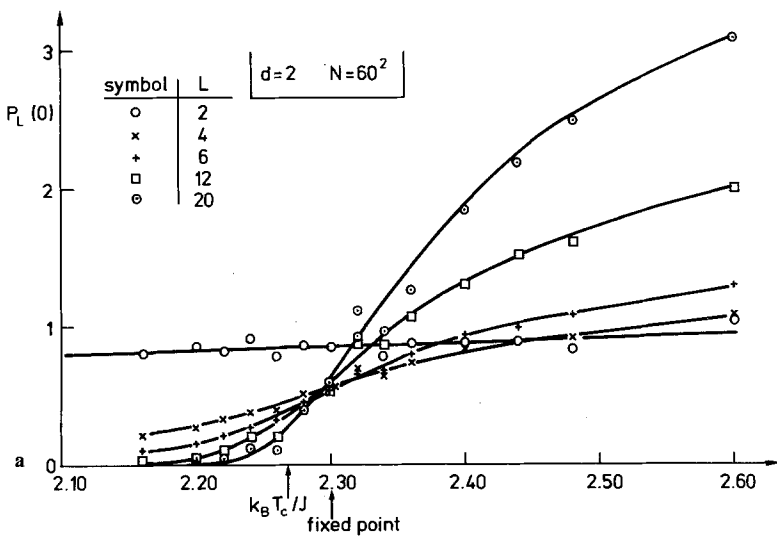
Fig. 5. Various extrapolations of block observables yielding the susceptibility of the three-dimensional Ising model at several temperatures. High temperature series estimates (HTS) [39] are indicated by arrows

(7), (9), $P_L(s=0)$ (15) or the half width Δs of the distribution, which we define from

$$P_L(s_{max} \pm \tfrac{1}{2}\Delta s) = P_L(s_{max})/2, \qquad (46)$$

and use (15) again; below T_c, one may analogously use (19), (20), $P_L(s_{max})$ (21) or again Δs. One notes from (5) that often various estimates are more or less nicely consistent with each other, though significantly different from the result for χ (known from high temperature series [39]). This fact indicates that the gaussian approximations (15a), (21) are reasonable, but it is important to take the difference between χ_L and χ into account (9), and hence find the true χ from an extrapolation linear in $1/L$, both above and below T_c. Only for the temperature closest to T_c shown here ($k_B T/J = 4.57$), the different methods for estimating χ_L disagree more distinctly, indicating that the distribution is distinctly nongaussian for the values of L considered, and hence here we are in a regime $L \lesssim \xi$ rather than $L \gg \xi$ needed for the linear extrapolation (9) to be valid. At this temperature, one hence cannot reliably extrapolate the data to find χ – but this fact is apparent from the behavior of the data themselves.

Figure 6 shows the temperature variation of $P_L(0)$. Since for large enough L $P_L(0)$ must increase with L for $T > T_c$ [Eq. (15)] but decrease with L for $T < T_c$ (42), a (rough) estimate of T_c is obtained from the temperature where these curves intersect. With free boundary conditions, the "effective" T_c of small blocks is shifted to distinctly lower temperatures, as expected [24, 29].
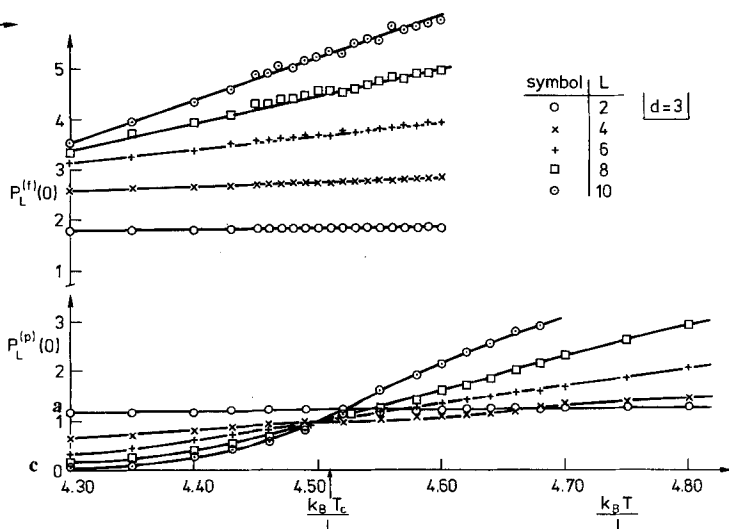

Fig. 6. Temperature variation of $P_L(0)$ for various L and $d=2$ (a), $d=3$ (b), as well as corresponding data for $P_L^{(f)}(0)$ and $P_L^{(p)}(0)$ (c). Estimates for T_c as well as estimates for the temperatures at which $P_L(s)$ exhibits fixed point behavior (Sect. IV) are included
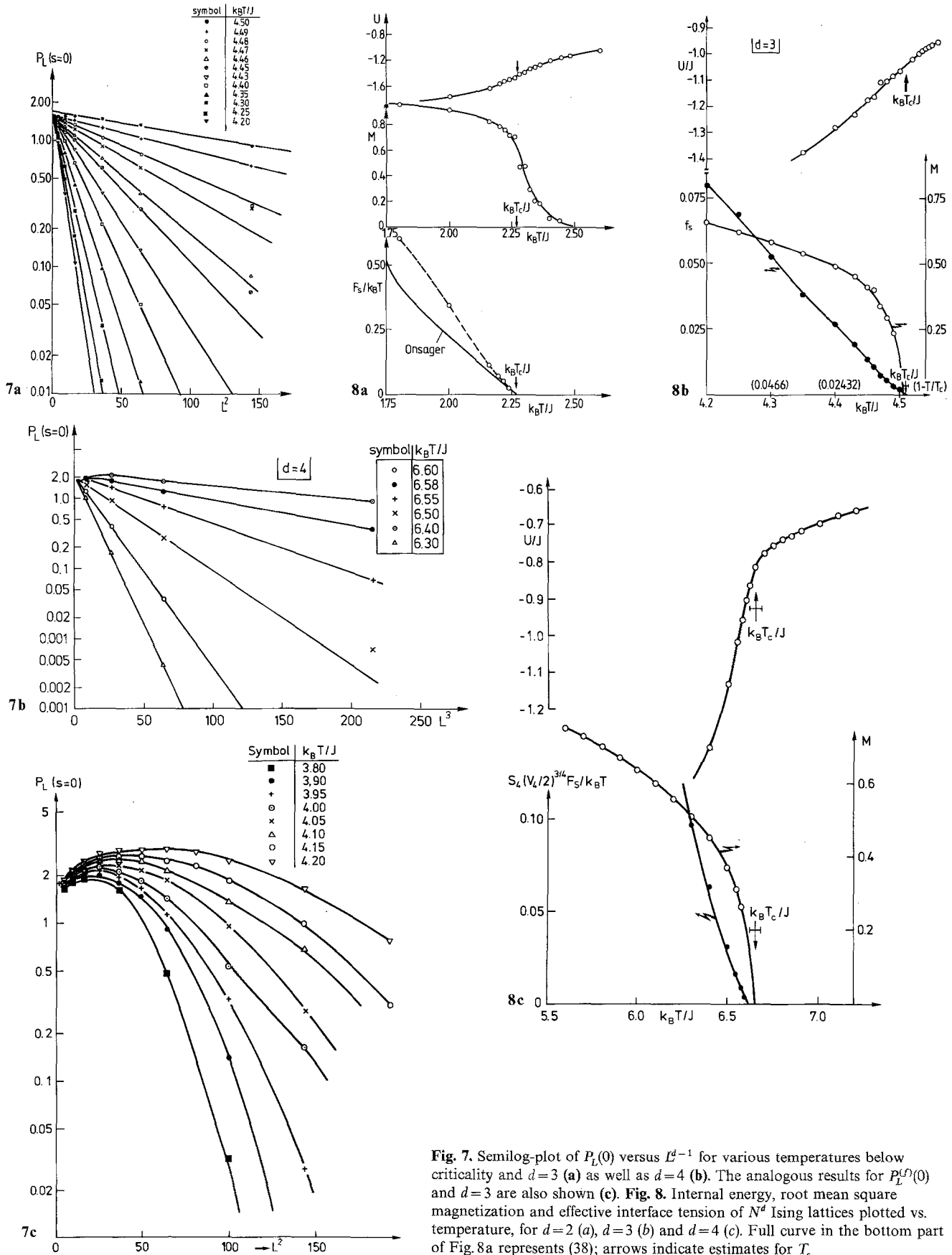
Fig. 7. Semilog-plot of $P_L(0)$ versus L^{d-1} for various temperatures below criticality and $d=3$ (**a**) as well as $d=4$ (**b**). The analogous results for $P_L^{(f)}(0)$ and $d=3$ are also shown (**c**). **Fig. 8.** Internal energy, root mean square magnetization and effective interface tension of N^d Ising lattices plotted vs. temperature, for $d=2$ (*a*), $d=3$ (*b*) and $d=4$ (*c*). Full curve in the bottom part of Fig. 8a represents (38); arrows indicate estimates for T_c

For finite systems with free or periodic boundary conditions, $P_L^{(f,p)}(s)$ as well as its moments are analytic at T_c, and this fact is also quite obvious from the data (Fig. 6c). For subsystem-blocks, however, the moment $\langle s^2 \rangle_L$ must have an energy-like singularity, since for L fixed it contains short-ranged correlations $\langle s_l s_{l'} \rangle_T$ only, (7), and hence (35) implies

$$\langle s^2 \rangle_L = L^{2\beta/\nu}(a^2 C_0)^{-1}$$
$$[f_2(\infty) - g_2(\xi/L)^{-(1-\alpha)/\nu} + - ...] \qquad (47a)$$

(subblocks)

where g_2 is a constant and α the specific heat exponent, while for free or periodic blocks analyticity in temperature implies

$$\langle s^2 \rangle_L^{(f,p)} = L^{2\beta/\nu}(a^2 C_0)^{-1} [f_2^{(f,p)}(\infty)$$
$$- g_2^{(f,p)}(\xi/L)^{-1/\nu} + - ...] \qquad (47b)$$

(isolated blocks)

This difference, which will turn out to be important for later analysis, shows up in the structure of $P_L(0)$ also, where the rapid variation with temperature in Fig. 6a, b reflects the existence of this energy-like singularity [which is somewhat smoothed out due to the finiteness of N, of course], in contrast to the case of isolated blocks studied in Fig. 6c.

The rapid decay of $P_L(s=0)$ for $T < T_c$ with decreasing temperature and/or increasing L reflects the exponential variation (42). This is seen more clearly in Fig. 7 where $\log P_L(s=0)$ is plotted vs. L^{d-1}. It appears, notably for $d=3$ and $d=4$, that (42) is accurate down to very small L (Fig. 7a, b). The same behavior was found to be true for periodic blocks, while for free blocks the behavior is more complicated due to the interfering free surface contributions and effects due to edges and corners, Fig. 7c.

Fitting straight lines to the points in Fig. 7a, b, one may extract an effective interface tension F_s from their slope. The temperature variation of this effective interface tension is shown in Fig. 8, together with the temperature variation of more common quantities such as (root mean square-) magnetization M or internal energy U of the system. The temperature where F_s vanishes gives again an estimate of T_c, which is of comparable accuracy as the more standard procedures of locating T_c by estimating where M vanishes or where U has an inflection point [10]. For $d=2$ and $d=3$, all these estimates are consistent with the accepted results $k_B T_c/J \cong 2.269$ ($d=2$) [37] and $k_B T_c/J \cong 4.510$ ($d=3$) [39], while for $d=4$ the smallness of N in this case ($N=12$) already leads to an appreciable shift of T_c, our estimate being $k_B T_c/$

$J \cong 6.65$ instead of $k_B T_c/J \cong 6.68$ [40]. In view of this fact, it seems doubtful to us whether previous studies of the $d=4$ Ising which did not take any shift of T_c into account [41] could verify the presence of logarithmic corrections to the mean-field power law behavior [42].

For $d=2$ the "effective interface tension" F_s estimated as described above can be compared with the exact result [37]

$$F_s = 2J - k_B T \ln\{(1 + e^{-2J/k_B T})/(1 - e^{-2J/k_B T})\}. \qquad (48)$$

While the agreement between the data and (48) is reasonable in the critical region, the effective surface tension estimated here is distinctly enhanced in comparison with (48) at lower temperatures. A similar enhancement of the surface tension of small droplets was found in direct simulations of the coexistence between small "critical clusters" and surrounding supersaturated lattice gas [28]. A more detailed analysis of this problem, as well as methods for obtaining reliably the standard interface tension associated with the infinite flat interface between bulk phases will be given elsewhere [43].

We next turn to a check of the finite size scaling assumption (32). We first consider the scaling of $P_L(0)$. Taking $\beta = 0.325$, $\nu = 0.630$ [8] and $k_B T_c = 4.51$ [39] and plotting $P_L(0) L^{-\beta/\nu}$ vs. $|1 - T/T_c|^{-\nu}/L$, the set of curves in Fig. 6b should "collapse" to a single curve $\tilde{P}(0, z')$. Figure 9a shows that this holds rather approximately, however, and systematic deviations are apparent. These systematic deviations may be entirely due to the use of too small L. We suspect, however, and this is corroborated by the analysis of Sect. IV, that at least part of the systematic deviation is due to the finiteness of N, which leads to slight shifts of T_c. The data shown in Fig. 9a correspond to the case $\xi/L > 1$, and hence corrections ξ/N cannot be completely disregarded. Anticipating the result of Sect. IV that the main result of these corrections is a 1%-shift of the effective T_c from $k_B T_c/J \cong 4.51$ to $k_B T_c^{\text{eff}}/J \cong 4.55$, Fig. 9b shows that now the data points scatter around a single curve, as expected from the scaling hypothesis.

It is also interesting to estimate the function $\tilde{P}(z, \infty)$, since a treatment of Bruce [10] using Wilson' approximate recursion relations [6] predicts pronounced dimensionality effects for $\tilde{P}(z, \infty)$. Figure 10 shows that for $d=3$ our results for $\tilde{P}(z, \infty)$ are not much affected by the uncertainty about T_c^{eff} – temperatures close to T_c do yield all (Fig. 10a, b) roughly the same scaled function, and the agreement with the prediction of Bruce is excellent! For $d=2$, the agreement is not as good (Fig. 10c): although we confirm the main point, that $\tilde{P}(z, \infty)$ has a pronounced double-peak structure, we do not find as
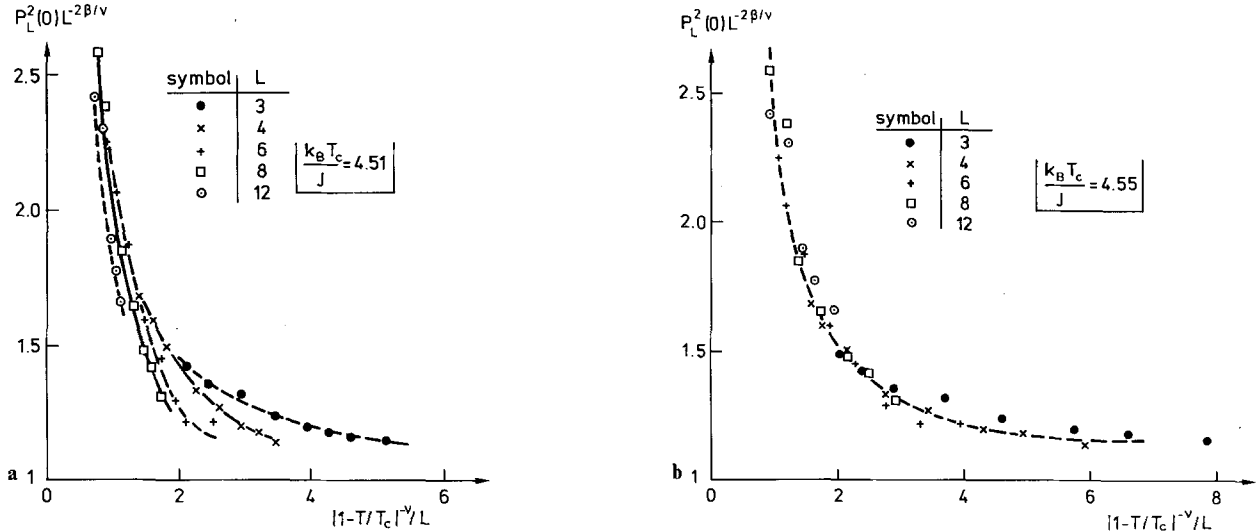
Fig. 9. Finite size scaling plot of $P_L^2(0)L^{-2\beta/\nu}$ versus $|1-T/T_c|^\nu/L$, for three-dimensional subblocks using either $k_B T_c/J = 4.51$ (a) or $k_B T_c^{eff}/J = 4.55$ (b)

rich a structure for small z, and also both peak height and position are somewhat different. This discrepancy may be due to one (or more) of the following reasons: *(i)* Due to the finite size of the lattice ($N = 60$) and/or finite computing time our results are not yet representative enough for the critical-point behavior of an infinite system. *(ii)* For $d = 2$ the methods of Reference 10 are not as reliable as for $d = 3$ *(iii)* The block distribution function at the critical point depends on the shape of the block. Reference 10 treats spherical blocks in momentum space, while we treat quadratic blocks in real space.

The last explanation seems the most likely to us, since we find that the block distribution function at criticality significantly depends on the boundary conditions of the block, Fig. 11. Due to the infinite correlation length at T_c, the effects due to the boundaries never become negligible, irrespective of the size of the block: thus the limit of the distribution function for $L \to \infty$ for subblocks, free and periodic blocks are all different, and it is plausible that different block shapes would also yield different block distribution functions. Such a behavior is possible since the limits $T \to T_c$ and $L \to \infty$ are not interchangeable. As a result, the "universality" of the finite size-scaling function $\tilde{P}(z, z')$ (32) is true only in a very restricted sense!

IV. Monte Carlo Renormalization Group (MCRG) Based on Block Distribution Functions

There have been a vast number of suggestions to utilize Monte Carlo methods for real-space renor-

malization group treatments [14–23, 44, 45]. The usual treatment again divides the system into blocks, but rather than allowing the block variable S_i to be quasi-continuous {as it actually is, see Sect. III, if one defines it by (1)}, one introduces a block-variable S_i' which has again Ising-like character, $S_i' = \pm 1$. Thus S_i' is not obtained by a coarse-graining as in (1) but by some more or less arbitrary projection operator $P(\{S_i\}, \{S_i'\})$ (majority rule, etc. [4–6]). Thus a new Hamiltonian $\mathscr{H}'(\{S_i'\})$ is constructed,

$$\exp\left[-\mathscr{H}'(\{S_i'\})/k_B T\right]$$
$$= \mathrm{Tr}_{\{S_i\}} P(\{S_i\}, \{S_i'\}) \exp\left[-\mathscr{H}(\{S_i\})/k_B T\right]. \tag{49}$$

Taking the trace in (49) one has to consider both the contribution of spins in the same block, as well as spins in different blocks producing an interaction between the blocks. A first step towards a MCRG is to do the first part (trace over spins within one block) by Monte Carlo, and treat the block-block interaction by cumulant expansion [45] or mean-field like approximations [44]. This approach has the merit that it is straightforward to apply to $d = 3$ or even higher dimensionality as well to arbitrary spin dimensionality [44], but clearly a meaningful accuracy has not been obtained so far.

More powerful is to consider the block-block interaction exactly for a system containing of two blocks only, where one can proceed to large blocks and perform an extrapolation to infinite block sizes [15]. Related extrapolations have also been performed for rather special renormalization group transformations appropriate for percolation [16] and random walk problems [21, 22].
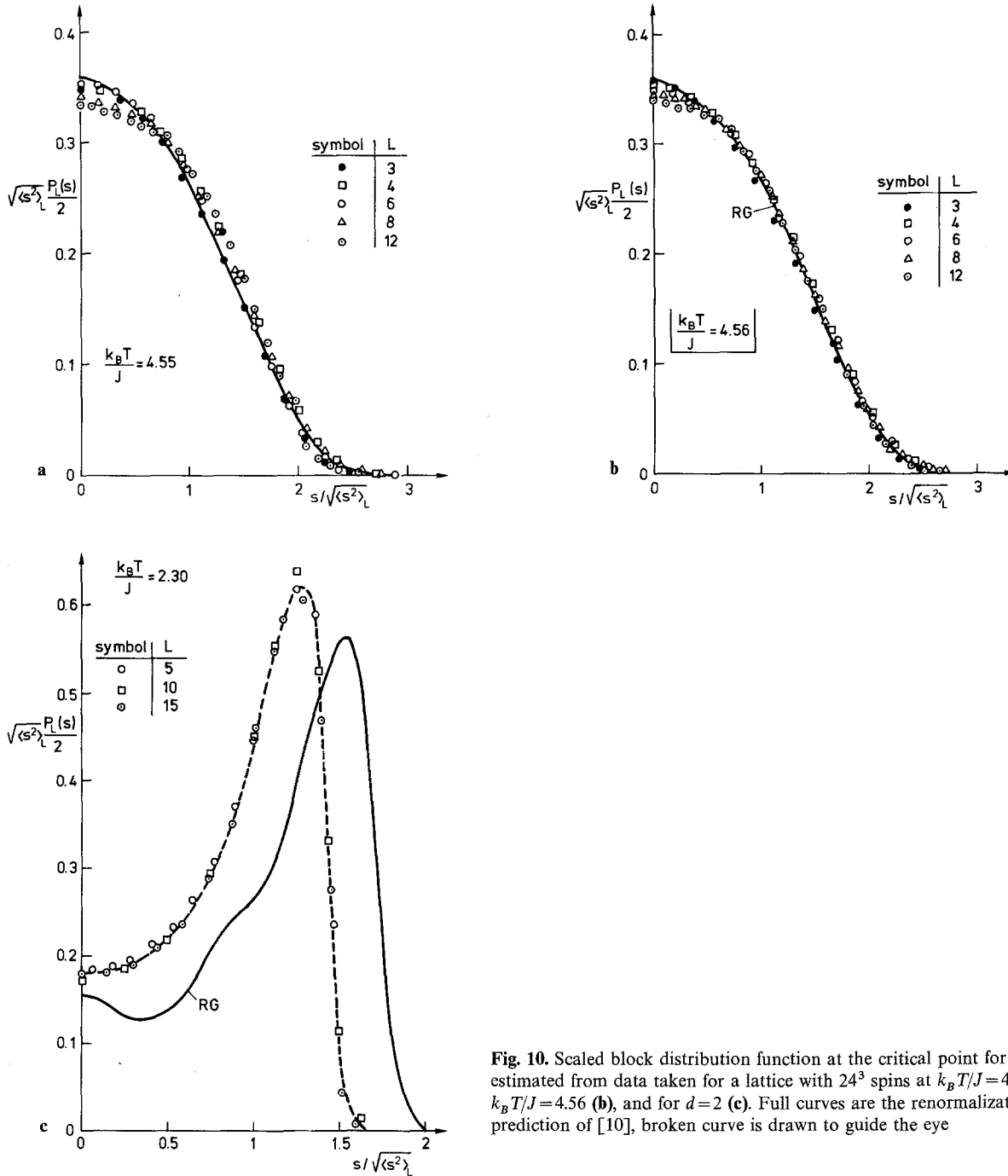
Fig. 10. Scaled block distribution function at the critical point for $d = 3$, estimated from data taken for a lattice with 24^3 spins at $k_B T/J = 4.55$ **(a)** and $k_B T/J = 4.56$ **(b)**, and for $d = 2$ **(c)**. Full curves are the renormalization group prediction of [10], broken curve is drawn to guide the eye

The most ambitious approach clearly is due to Ma [14] who tries to fit the fixed-point form of the block spin Hamiltonian, and includes also dynamic critical properties. However, the most successful applications are due to the approach of Swendsen [17–20], where one is concerned directly with the eigenvalues of the linearized renormalization group transformation near the fixed point Hamiltonian rather than with the fixed point Hamiltonian itself. Both approaches [14, 17–20] include all block-spin interactions (compatible with the finite size of the lattice), only in the analysis yielding the eigenvalues there is always some ambiguity concerning which block-spin interactions are included. In addition, the results are somewhat dependent on both the size of the blocks and the projection $P(\{S_i\}, \{S'_i\})$ [17], and hence it is hard to estimate reliably the errors of this procedure – though the errors seem to be encouragingly small [17–20].

Thus there is still some interest in constructing alternative MCRG procedures, particularly since none of the existing real-space renormalization group studies
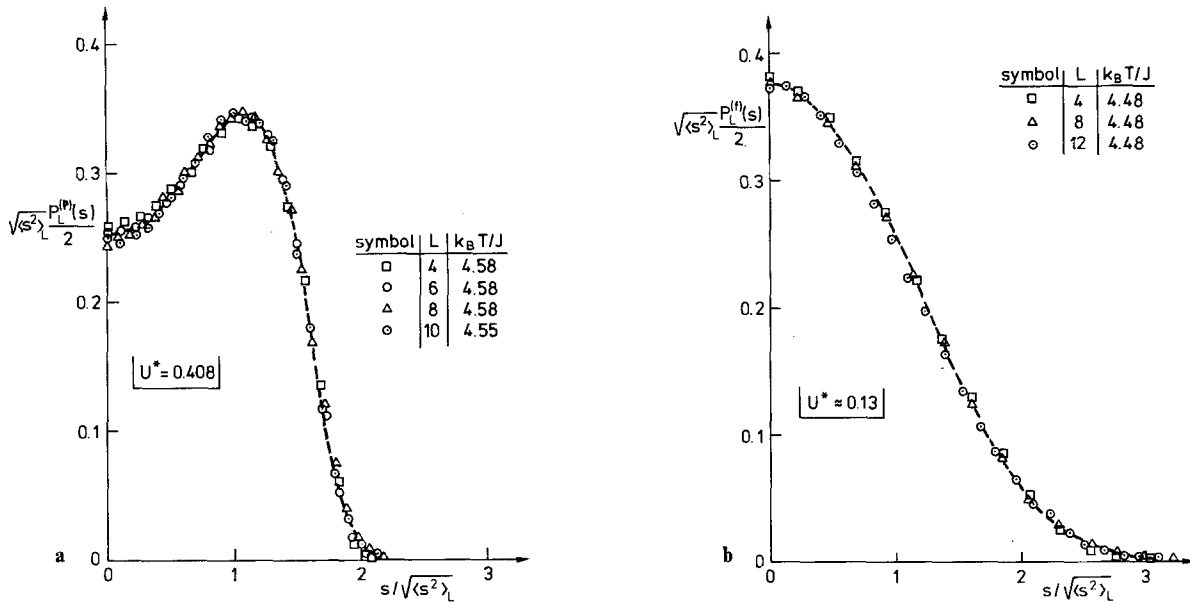
Fig. 11. Scaled block distribution function at criticality for three-dimensional blocks with periodic (**a**) and free (**b**) boundary conditions. The temperatures were chosen such that U_L equals the fixed-point value U^* expected from the treatment of Sect. IV
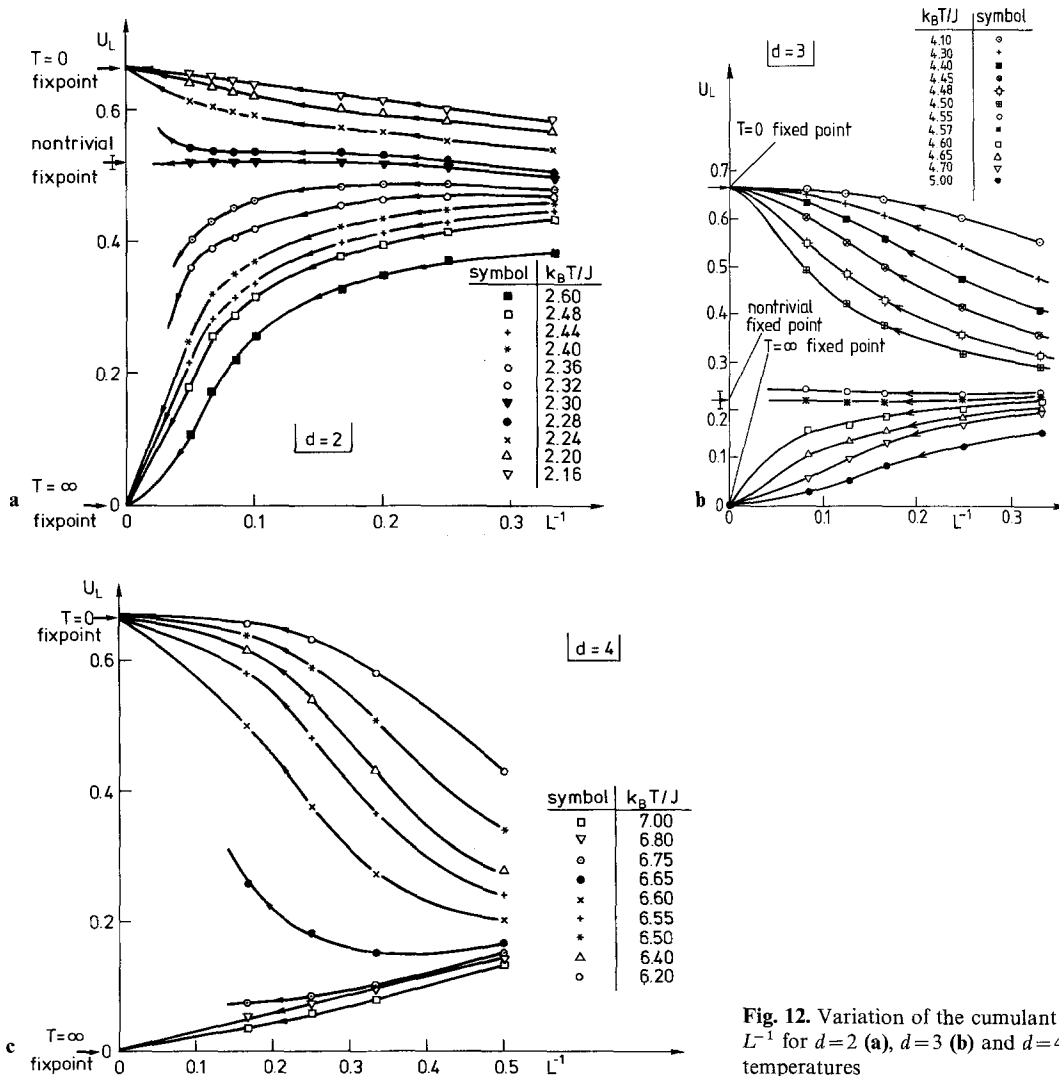

Fig. 12. Variation of the cumulant U_L with inverse block size L^{-1} for $d=2$ (**a**), $d=3$ (**b**) and $d=4$ (**c**) for various temperatures

allow for the occurrence of truly gaussian fixed points (apart from self-avoiding walk studies [21], where gaussian behavior trivially occurs for the non-self-avoiding walk). In addition, it is not clear that the existing schemes [14–23] are also powerful for systems with continuous degrees of freedom, such as the n-vector model, or even systems belonging to the Ising universality class as liquid-gas systems, or systems with structural phase transitions, which would also be interesting candidates for renormalization group studies [47].

The most complete approach along the lines developed in this paper would be to obtain the set of parameters $\{h_L, u_L, v_L, \ldots, C_L \ldots\}$ introduced in (4) and study their change upon a change of length scale L, and analyze the approach of $\mathscr{H}_{\mathrm{LGW}}$ to a nontrivial fixed point. This ambitious program cannot be based on a study of $P_L(s_i)$ alone, however, it would require studying the joint distribution function of two neighboring blocks i, j

$$P_L(s_i, s_j) = \int \prod_{k \neq i, j} ds_k P_L(\{s_k\}). \tag{50}$$

Of course, also $P_L(s)$ could be represented formally in a structure analogous to (3), (4),

$$P_L(s) = (1/Z') \exp[-\mathscr{H}'(s)],$$
$$\mathscr{H}'(s) = h'_L s + r'_L s^2 + v'_L s^4 + \ldots, \tag{51}$$

where $Z' = \int\limits_{-\infty}^{+\infty} ds \exp[-\mathscr{H}'(s)]$. Thus one can study the change of the parameters $\{h'_L, r'_L, v'_L, \ldots\}$ as a function of L. Although the nontrivial fixed point which is eventually reached when transformations from the length scale L to another length scale L' are performed is not the fixed point of the renormalization group transformation of $\mathscr{H}_{\mathrm{LGW}}$, one nevertheless can obtain the exponents from the behavior near the fixed point in an analogous fashion. Of course, the parameters $\{h'_L, r'_L, u'_L, v'_L, \ldots\}$ are uniquely related to the moments $\langle s^k \rangle_L$ {or cumulants U_L, V_L, etc., see (11), (12)} of the distribution function. While the set $\{h'_L, r'_L, u'_L, v'_L \ldots\}$ could be obtained from $P_L(s)$ only via extensive least-square fitting procedure, quantities such as $\langle s^2 \rangle_L, U_L, V_L, \ldots$ are a direct output of the calculation, and thus more convenient to use.

Hence the variation of quantities such as U_L, V_L, etc. with block size can be interpreted in analogy with a renormalization group "flow diagram", Fig. 12. Upon change of length scale, U_L reaches the trivial fixed point values $U^* = 0$ for temperatures above T_c, as expected (14), and $U^* = 2/3$ for temperatures below T_c (20). At the critical point itself, nontrivial values of U^* are reached for $d = 2$ and $d = 3$, as

expected from (37). From Fig. 12c it seems plausible that $U^* = 0$ for $T = T_c$ at $d = 4$, however, as expected for a critical behavior described by a gaussian fixed point. Of course, the smallness of N allowed us to study very small values of L only, and a study of larger systems would be very desirable to establish this point more convincingly.

Clearly, estimating the fixed point from the "flow diagram", Fig. 12, would not be a very accurate procedure. A more systematic method is to study the function $U_{L'} = U_{L'}(U_L)$, Figs. 13a, 14: estimates for the fixed point U^* result from the point where $U_{L'} = U_L$. If our values of L were large enough that corrections to the scaling forms (32), (37) are negligible, the estimates U_L^* for U^* should be independent of L. Due to corrections to scaling there is in fact, a slight dependence on L, which will be analyzed below. Here we draw attention to the fact that the function $U_{L'}(U_L)$ is a very smooth function throughout the critical region; in a wide environment of U_L^* it is well approximated by a straight line (for a global description of $U_{L'}(U_L)$ see Fig. 14a, left part, where all three fixed points are included). Thus rather accurate estimates for U_L^* can be obtained, without any influence of any ambiguity in locating T_c, estimating critical exponents, etc. In fact, plotting then the ratio $U_{L'}/U_L$ as a function of temperature, an estimate for T_c is obtained from the condition

$$(U_{L'}/U_L)_{T = T_c} = 1; \tag{52}$$

the estimate for T_c obtained in this way again is independent of any estimates for the critical exponents. Again we note that $U_{L'}/U_L$ is a rather smooth function of temperature, although one expects singularities similar to those described by (47a). In fact, if we perform the same procedure with free or periodic blocks, for which all moments $\langle s^k \rangle_L$ are analytic functions of temperature (47b), the variation of $U_{L'}/U_L$ with T is somewhat smoother (Fig. 13c).

Rather than studying $U_{L'}(U_L)$, one could study other moments such as $V_{L'}(V_L)$ as well: the scaling hypothesis implies analogous behavior for all moments. Of course, corrections to scaling would lead to systematic discrepancies between the estimates drawn from various moments, if L', L are finite. Actually the values of L', L chosen here are rather small, but Fig. 13c shows that the systematic discrepancy between the estimate $T_c^{(L)}$ for T_c drawn from $(U_{L'}/U_L)_{T_c} = 1$ and from $(V_{L'}/V_L)_{T_c} = 1$ is rather small – it is much smaller than the systematic dependence of $T_c^{(L)}$ on L itself. Thus the scaling form (32) is at least a reasonable approximation for all L down to $L = 3$ in the critical region, as expected from its direct analysis (Figs. 10, 11).
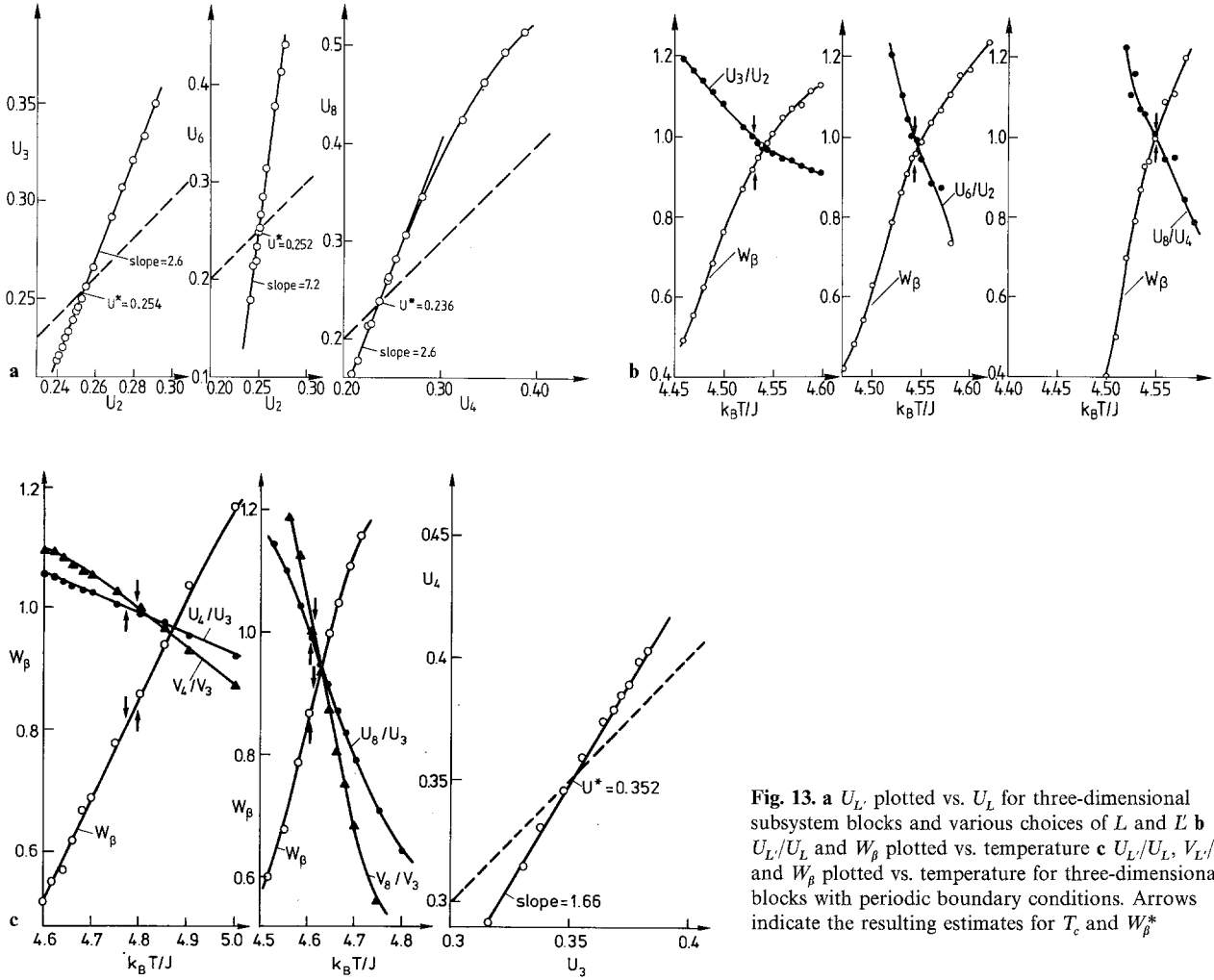
Fig. 13. **a** $U_{L'}$ plotted vs. U_L for three-dimensional subsystem blocks and various choices of L and L' **b** $U_{L'}/U_L$ and W_β plotted vs. temperature **c** $U_{L'}/U_L$, $V_{L'}/V_L$ and W_β plotted vs. temperature for three-dimensional blocks with periodic boundary conditions. Arrows indicate the resulting estimates for T_c and W_β^*
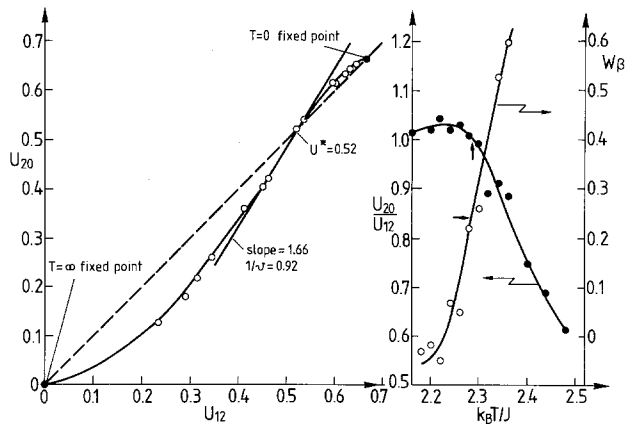

Fig. 14. U_{20} plotted vs. U_{12} for two-dimensional subsystem blocks (left part); U_{20}/U_{12} and W_β plotted vs. temperature (right part)

Estimating critical exponents is readily possible by a procedure very much analogous to Nightingale's phenomenological "finite size renormalization group" [11]. There one considers the scaling re-

lation for the correlation length $\xi_L(K)$ of a strip of width L in one direction and infinite in all other directions [$K \equiv J/T$]

$$\xi_L(K) = b \xi_{L/b}(K'). \tag{53}$$

These correlation lengths for models with discrete degrees of freedom (Ising-, Potts models etc.) can be obtained from transfer matrix methods. Equation (53) then yields implicitly the relation $K' = K'(K)$, and from the behavior at the fixed point K^* one obtains exponent estimates (such as $\partial K'/\partial K|K^* = b^{1/\nu}$ [11]). A direct use of this method in conjunction with Monte Carlo is impractical, of course: neither is it convenient to calculate strips which are verly large in one direction, nor is it easy to obtain the correlation length with sufficient accuracy. Rather than using (53) to study $K'(K)$, one can equally well use the function $U_{L'}(U_L)$, however. From (47) we obtain readily

$$U_L = U^* [1 - c_1 (\xi/L)^{-(1-\alpha)/\nu} + - \ldots],$$
$$\text{(subsystem blocks)} \quad (54a)$$

and

$$U_L = U^*_{(f,p)} [1 - c_1^{(f,p)} (\xi/L)^{-1/\nu} + - \ldots],$$
$$\text{(isolated blocks)} \quad (54b)$$

where c and $c_1^{(f,p)}$ are constants. Hence in the vicinity of U^* we have

$$\left. \frac{\partial U_{bl}}{\partial U_L} \right|_{U^*} \cong \frac{U_{bl} - U^*}{U_L - U^*} \cong \begin{cases} b^{(1-\alpha)/\nu} & \text{(subsystem blocks)} \\ b^{1/\nu} & \text{(isolated blocks)} \end{cases} \quad (55)$$

Thus the slope of the plot $U_{L'}(U_L)$ at U_L^* directly yields either the exponent $1/\nu$, as in the case of Nightingale's RG [11], or the exponent $(1-\alpha)/\nu = d - 1/\nu$. The latter value is a direct consequence of the singular temperature dependence of correlation functions of finite subsystem blocks near T_c, (47a).

From (35) we immediately can find the second critical exponent involved, by defining a function W_β:

$$W_\beta = -\ln [\langle s^2 \rangle_{bL} / \langle s^2 \rangle_L] / \ln b. \quad (56)$$

Since at T_c the dependence of $\langle s^2 \rangle$ on L has a simple power-law form, $\langle s^2 \rangle_L = L^{-2\beta/\nu} \dfrac{f_2(\infty)}{a C_0}$, the value W_β^* of W_β at the fixed point is an estimate for the exponent $2\beta/\nu$. Again the function W_β is a rather smooth function of U_L or temperature, Figs. 13, 14, and hence fairly accurate estimates for this exponent can be read off from the graphs. Note that no simultaneous fit to T_c, β and ν to the data is involved, as in the traditional finite size scaling analysis of Monte Carlo data [9, 24, 35].

From the examples shown in Figs. 13, 14 it is obvious that these exponent estimates are affected by some systematic dependences on L and scale factor $b = L'/L$, as expected since (32) should be true only asymptotically for $L \to \infty$. For obtaining accurate results, *corrections to scaling* in (32), (35), (47) etc. must be taken into account. Thus, (35) is replaced by

$$\langle s^k \rangle_L = \frac{L^{-k\beta/\nu}}{a^k C_0} - f_k \left(\frac{\xi}{L} \right) \left\{ 1 + L^{-w} f_{k,c} \left(\frac{\xi}{L} \right) + \ldots \right\}, \quad (57)$$

where w is an exponent describing corrections to scaling, and $f_{k,c}(\xi/L)$ is an associate scaling function. As a result, W_β^* becomes more complicated,

$$W_\beta^* = \frac{2\beta}{\nu} - \frac{1}{\ln b} \ln\{[1 + (bL)^{-w} f_{k,c}(\infty)] / [1 + L^{-w} f_{k,c}(\infty)]\}$$
$$\approx \frac{2\beta}{\nu} - \frac{L^{-w} f_{k,c}(\infty)}{\ln b} (b^{-w} - 1). \quad (58)$$

In order that the exponent $2\beta/\nu$ is not biased by any assumption about the exponent w, it is advisable to extrapolate W_β^* as a function of $(\ln b)^{-1}$, treating L as a parameter: (58) implies then that W_β^* should be linear in $(\ln b)^{-1}$ for large b, and the intercept for $(\ln b)^{-1}$ should also be independent of L. Figure 15a shows that this method gives consistent results: a unique value for $(2\beta/\nu)$ is in fact obtained, within our accuracy the extrapolation yields a result independent of L,

$$2\beta/\nu \approx 1.03 \pm 0.01 \quad (59)$$

The systematic dependence on $(\ln b)$ and L can be described by (58) reasonably well, as the upper part of Fig. 15a shows: there a function $(2\beta/\nu)_{\text{corr}}$ is defined by adding a term $L^{-w} f_{k,c}(\infty)(b^{-w} - 1)/\ln b$ as a correction term to W_β^* and fitting the parameters $w, f_{k,c}(\infty)$ such that the points "collapse" on a horizontal straight line. Unfortunately the fitted parameters do not seem to have much physical significance, as we obtain $f_{2,c}(\infty) \approx 0.35$, $w \approx 1.8$, which is an unexpectedly large value for the correction exponent (corresponding to small correction effects, a fortunate fact for our analysis). What we think happens is that for such small L as used here there are several correction terms simultaneously coming into play, whose net effect fortunately cancels to some extent, and hence is fitted by an unreasonably large exponent. We feel, however, that this fact does not invalidate our estimate (59) above, as one expects W_β^* to behave rather smoothly as function of $(\ln b)^{-1}$ for large b. Equation (59) is in very good agreement with the estimates of field theoretic renormalization [8], while the conjectured rational value $2\beta/\nu = 1$ ($\beta = 5/16$, $\nu = 5/8$) seems less likely, and the traditional value due to high temperature series expansions, $2\beta/\nu \approx 0.98$ [39], seems to be clearly ruled out. Our findings thus provide further evidence that the discrepancy between field-theoretic renormalization [8] and high-temperature series [39] should not be taken as an evidence that the discrete Ising model and continuum S^4-field theory belong to different universality classes, as suggested by Baker [32, 33]. We think that the quoted high temperature series result is unreliable due to too short series; recent series reanalysis are not inconsistent with this conjecture, although the accuracy of the series expansion estimates is still somewhat controversial [48, 49].

From (58) we note that the correct exponent $2\beta/\nu$ can be obtained either by extrapolation $\ln b \to \infty$ (as done here) or by extrapolation $L \to \infty$, $\ln b \to 0$, since then $(b^{-w} - 1)/\ln b = (e^{-w \ln b} - 1)/\ln b \approx -w$. If we hence choose, following Nightingale [11], $b = (L+1)/L$,
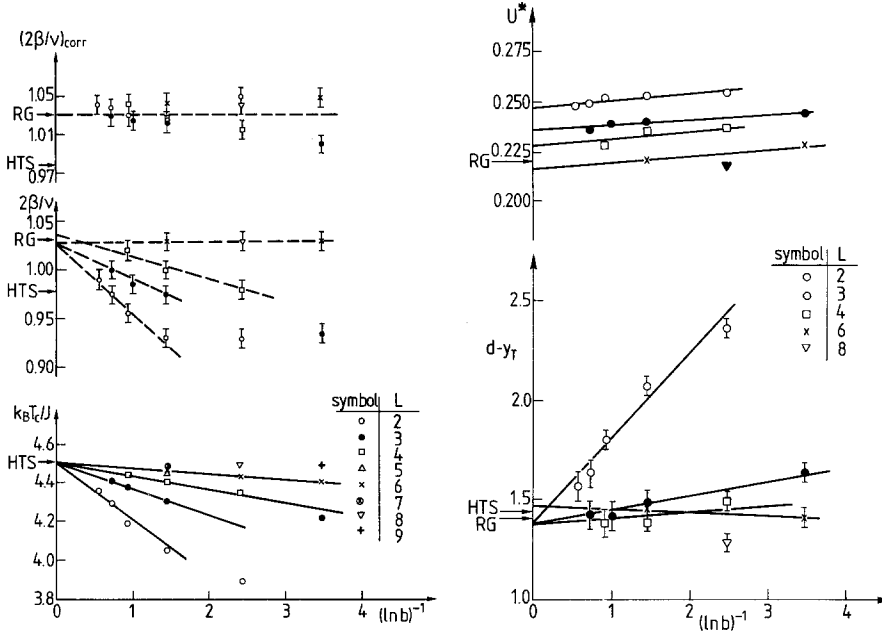
Fig. 15. a Estimates for $2\beta/\nu$ for three-dimensional subsystem blocks plotted vs. inverse logarithm of scale factor (middle part); estimates for $2\beta/\nu$ modified by fitting a correction term, cf. text (upper part); estimates for $k_B T_c/J$ for isolated blocks with free boundary conditions (lower part). **b** Estimates for U^* (upper part) and $(1-\alpha)/\nu = d - y_T$ for three-dimensional subsystem blocks (lower part)

one finds $W_\beta^* \approx \dfrac{2\beta}{\nu} + w f_{k,c}(\infty) L^{-w}$, i.e. the correction decreases in power-law form, and hence with increasing L the sequence of estimates W_β^* would be quickly convergent. We did not attempt to follow this method here, since very precise estimates for $\langle s_k \rangle_L$ are required to obtain W_β accurately enough.

From Figs. 15, 16, 17a it is seen that a systematic dependence on both scale factor b and linear dimension L not only affects the estimates for the exponents β/ν and $y_T = 1/\nu$ {or $d - y_T = (1-\alpha)/\nu$, respectively}, but the estimates for U^* and $k_B T_c/J$ as well, This fact is readily understood, generalizing (54) by including a correction term

$$U_L \approx U^*[1 - c_1(\xi/L)^{-(1-\alpha)/\nu} + L^{-w} f_{u,c}(\infty) + \ldots],$$
(subsystem blocks), $\qquad$ (60a)

$$U_L \approx U_{(f,p)}^*[1 - c_1^{(f,p)}(\xi/L)^{-1/\nu} + L^{-w} f_{u,c}^{(f,p)}(\infty) + \ldots],$$
$$\text{(isolated blocks)} \qquad (60\,\mathrm{b})$$

where the scaling function $f_{u,c}(\xi/L)$ involved in the correction term is approximated by $f_{u,c}(\infty)$ close to T_c. Now the fixed-point condition $U_L^* = U_{bL}^*$ is *not* satisfied for $\xi = \infty$, which would yield the bulk T_c, but rather the fixed-point condition is satisfied for a finite value of the correlation length ξ given by

$$\xi^{-(1-\alpha)\nu} = \frac{f_{u,c}(\infty)}{c_1} L^{-w-(1-\alpha)/\nu} \frac{b^{-1}-1}{\left(b^{\frac{1-\alpha}{\nu}}-1\right)},$$

$$\text{(subsystem blocks), (61\,a)}$$

or

$$\xi^{-1/\nu} = f_{u,c}^{(f,p)} L^{-w-1/\nu} \frac{b^{-w}-1}{b^{1/\nu}-1}, \quad \text{(isolated blocks). (61\,b)}$$

From (61) one easily obtains the expression for the shift ΔT_c between our estimate and the true T_c, remembering $\Delta T = T_c \xi^{1/\nu} \xi^{-1/\nu}$. From (61) we recognize the following facts: *(i)* $\Delta T_c \to 0$ for large b; for the values of b chosen in Figs. 15a, 16a one may, very roughly, approximate $b^{1/\nu} - 1$ by $\dfrac{1}{\nu} \ln b$, and hence the extrapolation of ΔT_c vs. $(\ln b)^{-1}$ is roughly linear; *(ii)* the shift decreases drastically with increasing L, this fact again being clearly borne out by the data.

By the same argument one can understand why the estimates for U^* (Figs. 15b, 16a) or V^* (Fig. 16b) do *not* converge to their asymptotic value independent of L, when being extrapolated vs. $(\ln b)^{-1}$. Equations (60), (61) imply instead

$$U_L^* = U^* \left[1 + L^{-w} f_{u,c}(\infty) \frac{1 - b^{-w-(1-\alpha)/\nu}}{1 - b^{-(1-\alpha)/\nu}}\right]_{b \to \infty}$$

$$\to U^*[1 + L^{-w} f_{u,c}(\infty)], \quad \text{(subsystem blocks)}, \qquad (62\,\mathrm{a})$$

or

$$U_L^* = U_{(f,p)}^* \left[1 + L^{-w} f_{u,c}^{(f,p)}(\infty) \frac{1 - b^{-w-1/\nu}}{1 - b^{-1/\nu}}\right]_{b \to \infty}$$

$$\to U_{(f,p)}^*[1 + L^{-w} f_{u,c}^{(f,p)}(\infty)], \quad \text{(isolated blocks). (62\,b)}$$

Since a quantitative fit of the above expressions to data involving values of L as small as $L = 2, 3$ (and
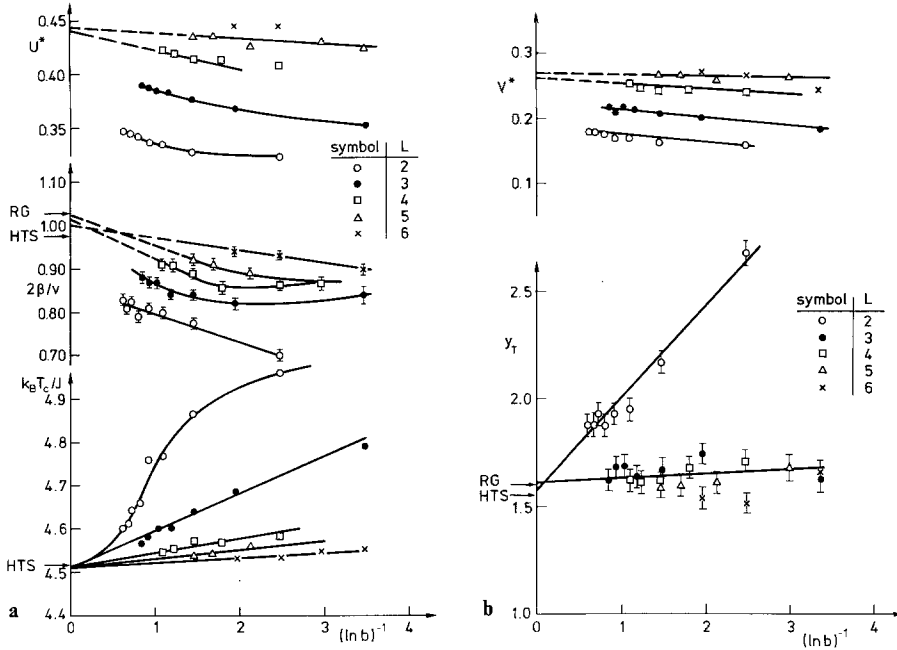
Fig. 16. a Estimates for U^* (upper part), $2\beta/v$ (middle part) and k_BT_c/J (lower part) for isolated three-dimensional blocks with periodic boundary conditions: b Estimates for V^* (upper part) and $y_T=1/v$ (lower part) for isolated three-dimensional blocks with periodic boundary conditions plotted vs. inverse logarithm of the scale factor
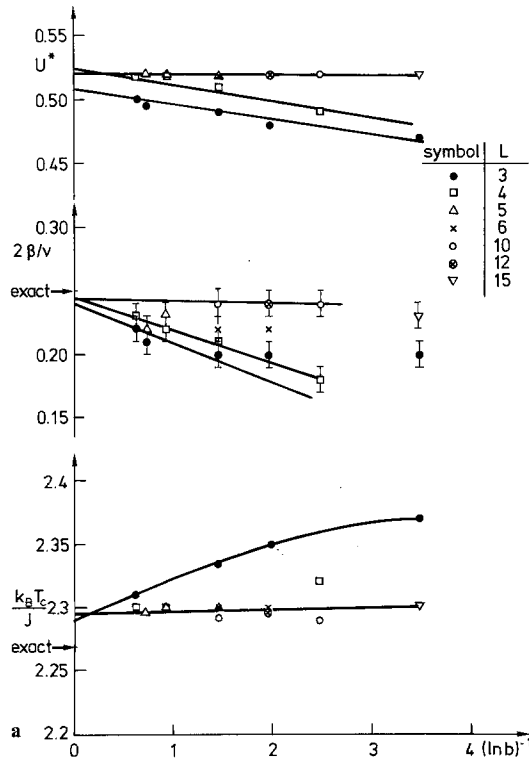

Fig. 17. a Estimates for U^* (upper part), $2\beta/v$ (middle part) and k_BT_c/J (lower part) for two-dimensional subsystem blocks plotted vs. inverse logarithm of scale factor; b W_β and U_3/U_2 (or U_4/U_2, respectively) plotted vs. temperature for four-dimensional subsystem plots (left part); resulting estimates for $2\beta/v$ (right part)

temperatures not always very close to T_c, which may lead to additional correction effects not considered here) seemed premature, we took as a final estimate for U^* the value U_L^*, for larger values of L where the systematic effects seem to disappear in the scatter of our data due to their limited statistical accuracy. Hence we obtain for subsystem blocks

$U^*\cong0.52\pm0.01\,(d=2),\qquad U^*\cong0.21\pm0.01\,(d=3)$ (63)

while for isolated three-dimensional blocks we get

$U_{(p)}^*\cong0.44\pm0.02,\qquad U_{(f)}^*\cong0.12\pm0.01.$ (64)

Equation (63) is in reasonable agreement with a treatment of Bruce [10] yielding $U^*\cong0.58$ $(d=2)$,

$U^* \cong 0.22$ ($d=3$), and are consistent with the direct scaling analysis of $P_L(s)$, see Sect. III.

While the estimates for T_c drawn from isolated blocks with either free (Fig. 15a) or periodic (Fig. 16a) boundary conditions are nicely convergent to the correct value for $(\ln b)^{-1} \to 0$, the estimates from subsystem blocks converge towards $k_B T_c/J \approx 4.55$ ($d=3$) rather than $k_B T_c/J \approx 4.51$ [39] and to $k_B T_c/J \approx 2.29$ ($d=2$) rather than to $k_B T_c/J \approx 2.269$ [37]. We interpret these 1%-discrepancies as finite-size effects due to the finiteness of our total lattice linear dimension, $N = 60$ ($d=2$) and $N=24$ ($d=3$). One does in fact expect a shift of the "effective" T_c of the rounded transition in the finite system of the order of $N^{-1/v}$ [29], yielding shifts of the order of 1% in our case. Unfortunately, in our case the proportionality constant in the relation $\Delta T_c/T_c \propto N^{-1/v}$ seems to be rather close to unity, while much smaller prefactors seem to apply when $\Delta T_c/T_c$ is defined from the specific heat maximum [29].

In view of these finite-size effects, it may be worthwhile to study subsystem blocks also for other values of N, to make sure whether there is any appreciable effect on the exponent estimates. From this point of view, the (less convenient) study of isolated blocks is superior – but there for the same values of L the correction effects due to the finiteness of L (such as included in (58)) are somewhat larger, and for reaching good enough accuracy blocks distinctly larger than $L=10$ (the maximum block size included in Fig. 16) is indispensable (for blocks with free boundary conditions the situation is even worse). Such a more extensive study, though feasible in principle, is not attempted here.

The exponent estimates obtained from the subsystem blocks are summarized as

$$2\beta/v = 1.03 \pm 0.01, \quad 1/v = 1.60 \pm 0.05 \quad (d=3), \quad (65\text{a})$$

$$2\beta/v = 0.24 \pm 0.02, \quad 1/v = 0.9 \pm 0.1 \quad (d=2). \quad (65\text{b})$$

For $d=4$ the same analysis (Fig. 17b) would yield $2\beta/v \approx 1.9$ rather than the answer $2\beta/v = 1$ appropriate for a gaussian fixed point. Since for $d=4$ logarithmic correction terms to the leading mean field behavior are predicted [42], the simple scaling analysis upon which our method for estimating exponents is based, must be reconsidered with great care; we are not pursuing this topic further since the smallness of N and L accessible for $d=4$ do not warrant such an analysis. The values $U_L^* > 0$ seen for small L (Fig. 17b) are nonzero only due to correction terms: we except $U^* = 0$, consistent with Fig. 12c, and then the exponents must be the mean-field exponents.
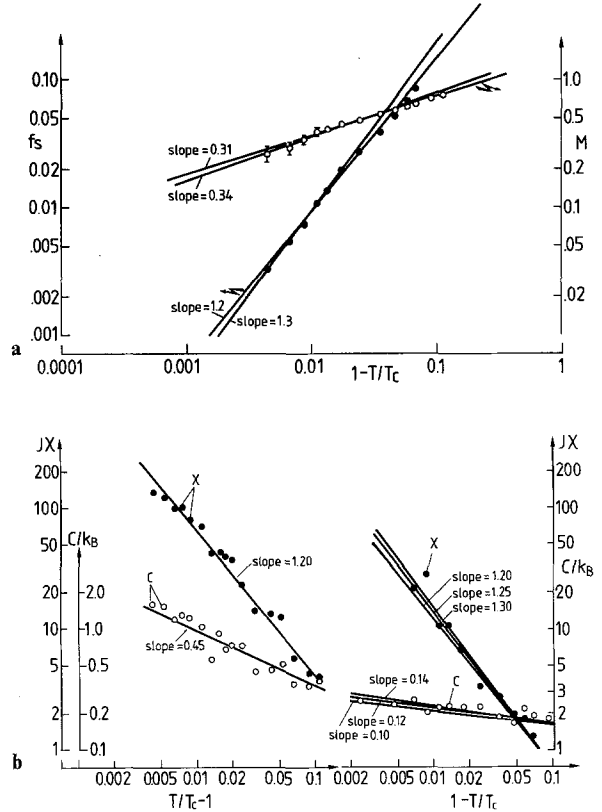

Fig. 18. a Magnetization M and "interface tension" f_s $= S_3 (V_3/2)^{1/3} F_s/k_B T$ of the three-dimensional Ising model plotted vs. $(1-T/T_c)$. b Specific heat C and susceptibility χ plotted vs. $T/T_c - 1$ (above T_c, left part) and $1 - T/T_c$ (below T_c, right part). Points are calculated from fluctuations of energy and magnetization, respectively, using about 10^2 statistically independent observations, taken at "time" intervals of about 50–100 MCS/spin for a system of 24^3 spins. $k_B T_c/J = 4,51$ was taken from high-temperature series [39]

We note that the exponent estimates drawn from three-dimensional isolated blocks with periodic boundary conditions and $L \leq 10$ would be $2\beta/v \approx 1.02 \pm 0.03$, $1/v = 1.60 \pm 0.05$, consistent with (65a), though the value of $2\beta/v$ is less accurate. Of course, the direct finite size scaling analysis of such small systems in the usual form [10, 24, 35] would yield by far more imprecise estimates. Similarly, if we analyze the Monte Carlo data of the systems used for the subsystem analysis in the standard way [10], i.e. by estimating exponents from log-log plots of all quantities in the critical region, we obtain rather imprecise estimates either, Figs. 18, 19: Even implying knowledge of T_c, the scatter of the data allows to "fit" straight lines with an uncertainty in the slope of several percent, e.g. for $d=3$ we find $\gamma = 1.25 + 0.05$, $\beta = 0.32 + 0.02$, $2v = 1.25 + 0.05$ (Fig. 18). More important, correction terms which sometimes are important can be masked in the scatter of data points completely, and hence from the slope of the
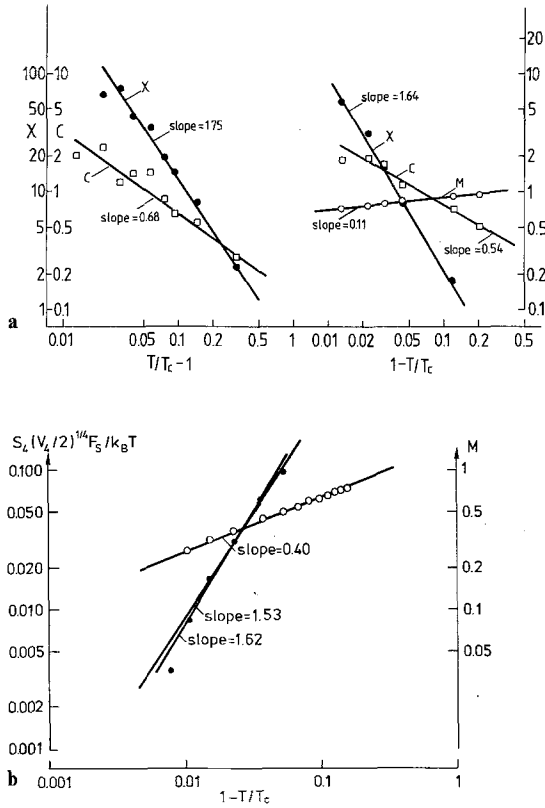
Fig. 19. a Magnetization M, susceptibility χ and specific heat C of the two-dimensional Ising model below T_c plotted vs. $(1 - T/T_c)$ (right part); specific heat C and susceptibility χ above T_c plotted vs. $T/T_c - 1$ (left part). Points are calculated from about 10^2 statistically independent observations taken at "time" intervals of about 50–100 MCS/spin for a system of 60^2 spins. $k_B T_c/J = 2.269$ was taken from the exact solution [37]; b "Interface tension" and magnetization of the four-dimensional Ising model plotted vs. $1 - T/T_c$

resulting "straight line" an estimate is obtained, which is definitely off: this happens for the specific heat above T_c, where $\alpha \approx 0.45$ ($d = 3$) and $\alpha \approx 0.68$ ($d = 2$) would result from such a naive analysis; disregarding logarithmic corrections at $d = 4$ leads to exponent estimates which are also systematically off, such as $\beta = 0.40$ instead of $\beta = 0.5$ (Fig. 19 b). In contrast, the above analysis of data obtained from the same runs takes effects due to correction terms in a systematic way into account, and hence the error bars quoted are much more reliable than those of the direct estimates from log-log plots.

V. Conclusions

In this paper, the probability distribution function $P_L(s)$ for observing an order parameter value s in a finite block of linear dimension L was discussed in detail for d-dimensional Ising models. It was shown

that for large L the properties of $P_L(s)$ can be interpreted in terms of the spontaneous magnetization M, susceptibility χ and interface tension F_s for temperatures T less than the critical temperature T_c, while above T_c $P_L(s)$ becomes simply a gaussian whose width determines the susceptibility χ. Right at T_c, $P_L(s)$ tends against a scaled universal form which is distinctly non-gaussian, and which depends strongly on the boundary conditions used (and presumably also somewhat on the shape of the block). For subsystem blocks we support the findings of Bruce, that $P_L(s)$ has a single peak at $s = 0$ at criticality for $d = 3$ while it is double-peaked for $d = 2$. For $d = 4$, $P_L(s)$ is also gaussian right at T_c.

A study of $P_L(s)$ in the context of Monte Carlo simulation can serve several purposes: first it was shown that reliable estimates of M, χ and F_s can be obtained; second, a Monte Carlo renormalization group analysis was proposed, from which one obtains exponent estimates much more accurately than from the standard fits to log-log plots; in fact, for $d = 3$ we could confirm the value $2\beta/\nu \approx 1.03$ from field-theoretic renormalization and reject the high-temperature series expansion estimate $2\beta/\nu \approx 0.98$. Since our analysis is based on an extrapolation vs. the inverse logarithm of the scale factor for various L, the *uniqueness* of the extrapolated result (being independent of L) proves the underlying (hyper-) scaling assumptions to be fully consistent with our data. This method takes corrections to scaling in a systematic way into account, and finite-size effects are well understood: particularly for isolated blocks with periodic boundary conditions, finite-size effects are the ingredients of the finite-size scaling description of $P_L(s)$, on which the "renormalization group" analysis is based. This method, which is related in spirit to the Nightingale phenomenological renormalization of finite strips, is hence an alternative to the Swendsen Monte Carlo renormalization group and reaches a comparable accuracy, particularly for three-dimensional systems. We emphasize that our method neither needs a-priori knowledge of the critical point nor extremely precise computations right at the critical point (which are hard to perform because of "critical slowing down", see [9]).

It should also be interesting to generalize this analysis to other quantities, e.g. the distribution $P_L(u)$ of internal energies u in a block. This quantity will tend towards a gaussian (both above and below T_c) centered at the internal energy U of the bulk system, the width being given by the specific heat. At T_c, we again expect a scaled universal form. From a Monte Carlo renormalization group analysis of $P_L(u)$ similar to the above one should be able to get additional estimates for α/ν and $1/\nu$, and hence obtain a further

check on the consistency of the analysis. $P_L(u)$ should also be useful for distinguishing second-order transitions from first-order transitions, where for large enough L a double-peaked structure of $P_L(u)$ must result which becomes sharper double-peaked with increasing L (while for second-order transitions near a tri-critical point a double-peak structure for smaller L must tend to a single-peak structure for large L).

Another possibility for future work along these lines would be the application to systems with continuous degrees of freedom. For example, for a liquid-gas system one would try to sample the block distribution function of density $P_L(\rho)$ in a grand-canonical simulation. Apart from the fact that $P_L(\rho)$ is no longer symmetric around $\rho = 1/2$ as in the lattice gas and that the chemical potential at criticality is non-trivial, the extension of the above methods should be straightforward. One thus could relate the liquid-gas critical point to the interatomic potential. More complicated but nevertheless promising would be the application to systems with n order parameter components where $P_L(S_1, \ldots, S_n)$ needs to be sampled. This task should at least be easy in fully symmetric cases, where one can instead consider $P_L\left(\sum_{i=1}^{n} s_i^2\right)$, such as in usual XY or Heisenberg models. We hope to report on such and similar application in the future.

References

1. Kampen, N.G. van: Phys. Rev. **135**, A362 (1964)
2. Kadanoff, L.P.: Physics **2**, 263 (1966)
3. Langer, J.S.: Ann. Phys. **65**, 53 (1971); Physica **73**, 61 (1974)
4. Langer, J.S., Baron, M., Miller, H.D.: Phys. Rev. A**11**, 1417 (1975)
   Billotet, C., Binder, K.: Z. Physik B – Condensed Matter **32**, 195 (1979)
5. Kawasaki, K., Imaeda, T., Gunton, J.D.: In: Studies in Statistical Mechanics. Raveche, H. (ed.). Amsterdam: North-Holland 1980
6. Wilson, K.G.: Phys. Rev. B**4**, 3174 (1971); B**4**, 3184 (1971)
7. Fisher, M.E.: Rev. Mod. Phys. **46**, 587 (1974)
   Domb, C., Green, M.S. (eds.): Phase Transitions and Critical Phenomena. Vol. 6. New York: Academic Press 1976
8. Le Guillou, J.C., Zinn-Justin, J.: Phys. Rev. B**21**, 3976 (1980)
9. Binder, K. (ed.): Monte Carlo Methods in Statistical Physics Berlin, Heidelberg, New York: Springer 1979
10. Bruce, A.D.: Preprint; see also Bruce, A.D., Schneider, T., Stoll, E.: Phys. Rev. Lett. **43**, 1284 (1979)
11. Nightingale, M.P.: Physica **83**A, 561 (1976); Proc. K. Ned. Acad. v. Wet. B**82** (3), 235 (1979)
12. Sneddon, L.: J. Phys. C**11**, 2823 (1978); C**12**, 3051 (1979)
    dos Santos, R.R., Sneddon, L.: Preprint
13. Racz, Z.: Phys. Rev. B**21**, 4012 (1980)
    Derrida, B., Vannimenus, J.: J. Phys. Lett. **41**, (1980)
    Derrida, B.: Preprint
    Nightingale, M.P., Blöte, H.W.J.: Physica **104**A, 352 (1980)
    Schick, M., Kinzel, W.: (unpublished)
    Blöte, H.W.J., Nightingale, M.P., Derrida, B.: Preprint
14. Ma, S.-K.: Phys. Rev. Lett. **37**, 461 (1976)
15. Friedman, Z., Felsteiner, J.: Phys. Rev. B**15**, 5317 (1977)
16. Reynolds, P.J., Stanley, H.E., Klein, W.: Phys. Rev. B**21**, 1223 (1980)
    Herrmann, H.J., Stauffer, D., Eschbach, P.D.: Phys. Rev. B**23**, 422 (1981)
17. Swendsen, R.H.: Phys. Rev. Lett. **42**, 859 (1979); Phys. Rev. B**20**, 2080 (1979)
18. Blöte, H.W.J., Swendsen, R.H.: Phys. Rev. B**20**, 2077 (1979)
19. Blöte, H.W.J., Swendsen, R.H.: Phys. Rev. B**22**, 4481 (1980)
20. Blöte, H.W.J., Swendsen, R.H.: Phys. Rev. Lett. **43**, 737 (1979)
    Swendsen, R.H., Krinsky, S.: Phys. Rev. Lett. **43**, 177 (1979)
    Rebbi, C., Swendsen, R.H.: preprint; Novotny, M.A., Landau, D.P., Swendsen, R.H.: Preprint
    Landau, D.P., Swendsen, R.H.: Preprint
21. Baumgärtner, A.: J. Phys. A**13**, L38 (1980)
    Kremer, K., Baumgärtner, A., Binder, K.: Z. Phys. B – Condensed Matter **40**, 331 (1981)
22. Redner, S., Reynolds, P.J.: Preprint
23. Shenker, S., Tobochnik, J.: Phys. Rev. B**22**, 4462 (1980)
24. Landau, D.P.: Phys. Rev. B**13**, 2297 (1976); B**14**, 255 (1976)
25. For connecting probability theory and renormalization group ideas, see Jona-Lasinio, G.: I. Nuovo Cimento **26**B, 99 (1975)
26. Binder, K., Rauch, H.: Z. Phys. **219**, 201 (1969)
27. Schulman, L.S.: J. Phys. A**13**, 237 (1980)
28. Binder, K., Kalos, M.H.: J. Stat. Phys. **22**, 363 (1980)
29. Fisher, M.E.: In: Critical Phenomena Green, M.S. (ed.), p.1. New York: Academic Press 1971
    Suzuki, M.: Prog. Theor. Phys. **58**, 1142 (1977)
30. The correlation length ξ, which enters the second argument of $\tilde{P}$ could differ from the standard definition of ξ by a constant of order unity. For simplicity this constant is here absorbed in the definition of ξ
31. Patashinskii, A.Z.: Sov. Phys. JETP **26**, 1126 (1968)
32. Baker, G.A., Jr.: Phys. Rev. B**15**, 1552 (1977)
33. Baker, G.A., Jr., Kincaid, J.M.: J. Stat. Phys. **24**, 469 (1981)
34. Stell, G.: In: Critical Phenomena. Green, M.S. (ed.), p.188. New York: Academic Press 1971
    Fisher, M.E.: In: Proceedings of the Twenty-Fourth Nobel Symposium on Collective Properties of Physical Systems. Lundquist, B., Lundquist, S. (eds.). p.16. New York: Academic Press 1973
35. Binder, K.: Thin Solid Films **20**, 367 (1974)
36. Baumgärtner, A., Binder, K.: J. Chem. Phys. (in press)
37. Onsager, L.: Phys. Rev. **65**, 117 (1944)
38. Because of the symmetry $P_L(s) = P_L(-s)$ only data for $s > 0$ are shown. The data in the figures arbitrarily are normalized to
    $\int_0^\infty P_L(s)\,ds = 1$ rather than 1/2
39. Domb, C.: In: Phase Transitions and Critical Phenomena. Vol. 3. Domb, C., Green, M.S. (eds.), Vol. 3. New York: Academic Press 1974
40. Gaunt, D.S., Sykes, M.F., McKenzie, S.: J. Phys. A**12**, 871 (1979)
41. Mouritsen, O.G., Knak Jensen, S.J.: Phys. Rev. B**19**, 3663 (1979)
42. Brezin, E., Le Guillou, J.C., Zinn-Justin, J.: Phys. Rev. D**8**, 2418 (1973)
43. Binder, K.: (to be published)
44. Kinzel, W.: Phys. Rev. B**19**, 4584 (1979)

45. Racz, Z., Rujan, P.: Z. Phys. B – Condensed Matter **28**, 287 (1977)
    Muto, S., Oguchí, T., Ono, I.: J. Phys. A**13**, 1799 (1980)
46. Leeuwen, J.M.J. van: In: Phase Transitions and Critical Phenomena. Vol. 6. Domb, C., Green, M.S. (eds.), Vol. 6. New York: Academic Press 1976
47. Müller-Krumbhaar, H.: Z. Phys. B – Condensed Matter (1980)
48. Nickel, B.G., Sharpe, B.: J. Phys. A**12**, 1819 (1979)
49. Gaunt, D.S., Sykes, M.F.: J. Phys. A**12**, L25 (1979)
    Rehr, J.J.: J. Phys. A**12**, L179 (1979)

McKenzie, S.: J. Phys. A**12**, L185 (1979)
Zinn-Justin, J.: J. Phys. (Paris) **40**, 969 (1979)

Kurt Binder
Institut für Festkörperforschung
Kernforschungsanlage Jülich GmbH
Postfach 19 13
D-5170 Jülich 1
Federal Republic of Germany

Note Added in Proof

For Ising systems with finite susceptibility it has been proven rigorously that the fixed-point Hamiltonian for the block spin. case is independent Gaussians [50]. This is consistent with the gaussian forms of the distribution chosen here off criticality. It should also be noted that the concept of obtaining a fixed-point probability distribution function in a real-space renormalization has also been used in the context of percolation studies [51]. Finally we mention that unintentionally it is not the order parameter distribution $P_L(s)$ as defined in (3), which was studied numerically in Sect. II, but a slightly different distribution $P_L'(s)$. In terms of the M states $\{s_i^{(L)}\}$ generated for the block variable these distributions can be expressed as $P_L(s) = (1/M) \sum\limits_{i=1}^{M} \delta(s_i^{(L)} - s)$ and $P_L'(s) = (1/M) \sum\limits_{i=1}^{M} \delta(s_i^{(L)} - s)/W(s_i^{(L)})$, where $W(s_i^{(L)})$ is the transition probability (for a single spin-flip) in state $s_i^{(L)}$. Since $W(s)$ is a very smooth function of its argument, the distributions $P_L(s)$ and $P_L'(s)$ are qualitatively similar, and tend towards the same distribution for large L. Since both distributions hence must have the same scaling behavior as $L \to \infty$, $T \to T_c$, they are equally well suited for the analysis presented in the paper.

50. Newman, C.M.: Commun. Math. Phys. **74**, 119 (1980); Baker, G.A., Krinsky, S.: J. Math. Phys. **18**, 590 (1977)
51. Stinchcome, R.B., Watson, B.P.: J. Phys. C**9**, 3221 (1976)